

PAPER-BASED ARRAYS FOR GEOGRAPHICAL INDICATION OF TURMERICS



A Dissertation Submitted in Partial Fulfillment of the Requirements
for the Degree of Doctor of Philosophy in Chemistry

Department of Chemistry

FACULTY OF SCIENCE

Chulalongkorn University

Academic Year 2019

Copyright of Chulalongkorn University

แนวลำดับฐานกระดาษสำหรับข้อบ่งชี้ทางภูมิศาสตร์ของขมิ้นชัน



น.ส.มนรวิศ รวยธนพานิช

วิทยานิพนธ์นี้เป็นส่วนหนึ่งของการศึกษาตามหลักสูตรปริญญาวิทยาศาสตรดุษฎีบัณฑิต

สาขาวิชาเคมี ภาควิชาเคมี

คณะวิทยาศาสตร์ จุฬาลงกรณ์มหาวิทยาลัย

ปีการศึกษา 2562

ลิขสิทธิ์ของจุฬาลงกรณ์มหาวิทยาลัย

มนรวีส รวยธนพานิช : แถวลำดับฐานกระดาษสำหรับข้อบ่งชี้ทางภูมิศาสตร์ของขมิ้นชัน. (PAPER-BASED ARRAYS FOR GEOGRAPHICAL INDICATION OF TURMERIC) อ.ที่
 ปริญญาหลัก : รศ. ดร.ธนัชฐ์ ปราณีนรารัตน์

การระบุสิ่งบ่งชี้ทางภูมิศาสตร์เริ่มมีบทบาทอย่างมากและถูกนำมาใช้เป็นเครื่องมือทางการตลาดเพื่อยกระดับและเพิ่มมูลค่าของสินค้าโดยเฉพาะอย่างยิ่งในด้านอาหาร งานวิจัยนี้ต้องการพัฒนาวิธีการทางวิทยาศาสตร์วิธีใหม่เพื่อใช้ระบุสิ่งบ่งชี้ทางภูมิศาสตร์ของขมิ้นชันซึ่งเป็นพืชสมุนไพรที่มีความสำคัญและเป็นองค์ประกอบที่สำคัญของอาหารในหลายภูมิภาค โดยใช้พื้นฐานจากปฏิกิริยาทางเคมีบนกระดาษร่วมกับการวิเคราะห์ข้อมูลด้วยเคโมเมตริกซ์ โดยหลักการสำคัญในการแยกความแตกต่างของขมิ้นชันที่มาจากแหล่งต่าง ๆ นั้น อาศัยความแตกต่างของสัดส่วนของสารประกอบที่พบในตัวอย่างขมิ้นจากแต่ละแหล่ง โดยสารกลุ่มหลัก ได้แก่ เคอร์คูมิน และสารอนุพันธ์ของเคอร์คูมิน ซึ่งยืนยันจากการศึกษาเบื้องต้นด้วยเทคนิค HPLC และ LC-MS นอกจากนี้ความแตกต่างของสารประกอบหลักและสารประกอบรองอื่น ๆ ก็จะมีผลต่อความไวและรูปแบบในการเกิดผลิตภัณฑ์กับรีเอเจนต์ต่างชนิดกันอีกด้วย ซึ่งทั้งหมดได้ถูกนำมารวมเป็นอุปกรณ์แถวลำดับฐานกระดาษ โดยมีรีเอเจนต์ที่ทราบว่าจะเกิดปฏิกิริยากับเคอร์คูมิน ได้แก่ สารละลายบัพเฟอร์, 2,4-ไดไนโตรฟีนอลไฮดรอกซี, วานิลิน และสารละลายไอออนของโลหะต่าง ๆ เมื่อรีเอเจนต์เหล่านี้เกิดปฏิกิริยากับสารประกอบในขมิ้นชันจะเกิดเป็นสารผลิตภัณฑ์ที่ทำให้เกิดการเปลี่ยนแปลงสีและฟลูออเรสเซนส์ของแถวลำดับฐานกระดาษที่มีเอกลักษณ์เฉพาะตัว การเปลี่ยนแปลงเชิงแสงเหล่านี้สามารถเก็บข้อมูลได้โดยใช้อุปกรณ์พื้นฐาน ได้แก่ เครื่องสแกนเนอร์และกล้องดิจิทัล ข้อมูลภาพนี้จะถูกนำมาแปลงเป็นข้อมูลตัวเลขเพื่อใช้วิเคราะห์ทางเคโมเมตริกซ์ต่อไป ผลการทดลองพบว่า เราสามารถหาความถูกต้องในการระบุแหล่งที่มาของตัวอย่างโดยใช้ข้อมูลจากแต่ละรีเอเจนต์มาผสมกันได้ทั้งสิ้น 2047 ชุดข้อมูล และพบว่าชุดข้อมูลที่ดีที่สุดสามารถระบุแหล่งที่มาของขมิ้นชันได้อย่างถูกต้องถึง 94% โดยไม่จำเป็นต้องใช้เครื่องมือระดับสูงอื่น ๆ เพิ่มเติม

สาขาวิชา เคมี
 ปีการศึกษา 2562

ลายมือชื่อนิสิต
 ลายมือชื่อ อ.ที่ปรึกษาหลัก

5972835823 : MAJOR CHEMISTRY

KEYWORD: geographical indication, turmeric, curcumin, paper-based device,
chemometrics

Monrawat Rauytanapanit : PAPER-BASED ARRAYS FOR GEOGRAPHICAL
INDICATION OF TURMERIC. Advisor: Assoc. Prof. THANIT PRANEENARARAT, Ph.D.

Geographical indications have gained increasing importance as a powerful marketing tool for highly valuable products especially foods. In this study, a synergistic combination of chemical reaction arrays on paper and chemometric analysis was used to uncover geographical indication of turmeric, an important food ingredient in several Asian cuisines. The key to effective differentiation was from the subtle differences in the compositions of the compounds found in turmeric samples, mainly curcumin and derivatives which were preliminarily confirmed by HPLC and LC-MS experiments. In addition, the differences in the major and minor components affect the reactivity and the pattern of obtained products after reacting with various types of reagents. Our paper-based arrays were fabricated based on the reactions of curcumin with various reagents including buffer solutions, 2,4-dinitrophenylhydrazine, vanillin and some metal ion solutions. The chemical sensors reacted with various components in turmeric in different ways and resulted in different colorimetric and fluorescence profiles. The photophysical changes of the arrays were simply captured using basic tools including a document scanner and a digital camera. The images were transformed into numerical data, which were then analyzed by chemometrics. As a result, geographical prediction from 2047 combinations of sensor were investigated and our strategy could select the best combination of reagents that provided up to 94% prediction accuracy without the need for any sophisticated instruments.

Field of Study: Chemistry

Student's Signature

Academic Year: 2019

Advisor's Signature

ACKNOWLEDGEMENTS

I would first like to thank my thesis advisor Associate Professor Dr.Thanit Praneenararat of the Department of Chemistry, Faculty of Science, Chulalongkorn University for his kind supervision and motivation during the study. His guidance and encouragement always make me feel warm since the beginning of my first project to present.

Besides my advisor, I would like to thank Associate Professor Dr.Kanet Wongravee and Ms.Thanyada Sukmanee of the Sensor Research Unit (SRU), Department of Chemistry, Faculty of Science, Chulalongkorn University for their endless help and support in Chemometrics.

My sincere thanks also go to my thesis committee for their very valuable questions and comments on this thesis and the Development and Promotion of Science and Technology Talented Project (DPST) for financial supports.

Finally, I would like to express my bottomless love and thanks to my family, my friends and all members in TP lab for providing me with continuous support throughout many years of the study. This accomplishment would not have been possible without them.

จุฬาลงกรณ์มหาวิทยาลัย
CHULALONGKORN UNIVERSITY

Monrawat Rauytanapanit

TABLE OF CONTENTS

	Page
ABSTRACT (THAI).....	iii
ABSTRACT (ENGLISH).....	iv
ACKNOWLEDGEMENTS.....	v
TABLE OF CONTENTS.....	vi
LIST OF TABLES.....	ix
LIST OF FIGURES.....	x
LIST OF ABBREVIATIONS.....	12
CHAPTER I INTRODUCTION.....	14
1.1 Geographical indication using chemical methods.....	14
1.1.1 Chromatographic techniques.....	14
1.1.1.1 High-performance liquid chromatography (HPLC).....	15
1.1.1.2 Gas chromatography (GC).....	15
1.1.2 Spectroscopic techniques.....	16
1.1.2.1 Nuclear magnetic resonance (NMR) spectroscopy.....	16
1.1.2.2 Ultraviolet-visible (UV-Vis) spectroscopy.....	16
1.1.3. Miscellaneous techniques.....	17
1.1.3.1 Sensory analysis.....	17
1.1.3.2 Electronic nose technology.....	17
1.2 Curcumin.....	19
1.2.1 pH sensing.....	20
1.2.2 Metal ions sensing.....	21

1.2.2.1 Boron sensing	21
1.2.2.2 Iron sensing	21
1.2.2.3 Lead sensing	22
1.3 Chemometrics	23
1.3.1 Unsupervised pattern recognition	23
1.3.1.1 Cluster Analysis (CA)	23
1.3.1.2 Principal Component Analysis (PCA)	24
1.3.2 Supervised pattern recognition	25
1.3.2.1 Linear Discriminant Analysis (LDA)	25
1.4 Purpose of this study	27
CHAPTER II EXPERIMENTAL SECTION	28
2.1 Materials and chemicals	28
2.2 Extraction procedure	30
2.3 Determination of main components in turmeric extracts	31
2.3.1 High-performance liquid chromatography (HPLC)	31
2.3.2 Liquid chromatography – tandem mass spectrometry (LC-MS)	31
2.4 Fabrication of paper arrays	33
2.5 Chemometrics	36
CHAPTER III RESULTS AND DISCUSSION	37
3.1 Determination of main components in turmeric extracts	37
3.2 Chemical detection on paper arrays	54
3.3 Chemometric analysis	65
CHAPTER IV CONCLUSION	71
REFERENCES	72

VITA..... 77



จุฬาลงกรณ์มหาวิทยาลัย
CHULALONGKORN UNIVERSITY

LIST OF TABLES

	Page
Table 1 The origins of turmeric samples used in this study.	29
Table 2 All reagents used in the paper arrays.	34
Table 3 Curcumin concentrations in methanol extracts of turmeric from different sources (at 426 nm, 3 replicates).	38
Table 4 HPLC chromatograms of methanol extracts from different sources of turmeric (at 250 nm).	39
Table 5 Peak identifications of a methanol extract from Cur2.	43
Table 6 Peak identifications of a methanol extract from Cur2 after reacting with DNP.	48

LIST OF FIGURES

	Page
Figure 1 The chemical structures of curcumin and common derivatives	19
Figure 2 Tautomeric forms of curcumin.	20
Figure 3 Chemical structure of rosocyanine complex.	21
Figure 4 Proposed mechanism for the Fe ²⁺ ions binding to curcumin.	22
Figure 5 An example of HCA dendrogram. ⁶	24
Figure 6 An example of two-dimensional PC score plot. ⁶	25
Figure 7 The pattern of the arrays used in this study.....	33
Figure 8 Calibration plot of peak areas of curcumin standard from HPLC experiment	37
Figure 9 Relative abundance of main components in turmeric extracts (at 250 nm). 45	
Figure 10 HPLC chromatograms of methanol extracts from (A) Cur2 and (B) Cur3 before and after reacting with DNP (at 250 nm).	47
Figure 11 Proposed mechanism for the hydrazone formation and subsequent condensation of curcumin.....	53
Figure 12 Paper arrays of chemical reactions probe after reacting with curcumin standard (Cur11) under (A) white light and (B) 365-nm UV light.	54
Figure 13 Paper arrays of chemical reactions probe after reacting with turmeric samples from all sources under (A) white light and (B) 365-nm UV light	55
Figure 14 Colorimetric and fluorescence responses of paper arrays to various reagents after being exposed to 0.2-mM curcumin standard (Cur11).....	57
Figure 15 Colorimetric responses of curcumin standard (Cur11) with different concentration of DNP and calibration plots of the Δ of mean color intensity.....	58

Figure 16 Colorimetric responses of curcumin standard (Cur11) with different concentration of vanillin and calibration plots of the Δ of mean color intensity	59
Figure 17 Colorimetric responses of curcumin standard (Cur11) with different concentration of H_3BO_3 and calibration plots of the Δ of mean color intensity.....	60
Figure 18 Colorimetric responses of curcumin standard (Cur11) with different concentration of Cu^{2+} and calibration plots of the Δ of mean color intensity	61
Figure 19 Colorimetric responses of curcumin standard (Cur11) with different concentration of Fe^{2+} and calibration plots of the Δ of mean color intensity.....	62
Figure 20 Colorimetric responses of curcumin standard (Cur11) with different concentration of Ni^{2+} and calibration plots of the Δ of mean color intensity.....	63
Figure 21 Colorimetric responses of curcumin standard (Cur11) with different concentration of Pb^{2+} and calibration plots of the Δ of mean color intensity.....	64
Figure 22 A plot between the percentages of prediction accuracies and the numbers of reagents used in the differentiation process.	66
Figure 23 Two-dimensional PC score plots of (A) PC1 vs. PC2 and (B) PC1 vs. PC3 for the combination of all reagents in discriminating 11 turmeric sources.	68
Figure 24 Two-dimensional PC score plots of (A) PC1 vs. PC2 and (B) PC1 vs. PC3 for the combination of 8 reagents (H_2O + pH2 + DNP + vanillin + H_3BO_3 + Fe^{2+} + Ni^{2+} + Pb^{2+}) in discriminating 11 turmeric sources.....	69
Figure 25 A heat-map chart as a representation of correctness in predicting the origins of turmeric samples.....	70

LIST OF ABBREVIATIONS

CA	Cluster Analysis
CE	Collision energy
CVA	Canonical variate analysis
CURNs	Curcumin nanoparticles
DAD	Diode-array detector
DNP	2,4-dinitrophenylhydrazine
DP	Declustering potential
FID	Flame ionization detector
GC	Gas chromatography
GI	Geographical indication
HCA	Hierarchical Cluster Analysis
HPLC	High-performance liquid chromatography
HPLC-DAD	High-performance liquid chromatography with a photodiode array detector
LC	Liquid chromatography
LC-MS	Liquid chromatography – tandem mass spectrometry
LDA	Linear Discriminant Analysis
LOD	Limit of detection
MS	Mass spectrometry
<i>m/z</i>	Mass-to-charge ratio
NMR	Nuclear magnetic resonance spectroscopy
PC	Principal Component
PCA	Principal Component Analysis
PLSDA	Partial least squares discrimination analysis
QTOF	Quadrupole time-of-flight
RGB	Red, green and blue
RT	Retention time
rt	Room temperature

SE	Standard error
TLC	Thin-layer chromatography
UHPLC	Ultra high-performance liquid chromatography
UV-Vis	Ultraviolet-visible



CHAPTER I

INTRODUCTION

1.1 Geographical indication using chemical methods

Geographical indications (GI), or signs used to indicate a clear link between an attribute and the origin of a product, have become an important tool for the economies of communities producing highly desired products.¹⁻² Prosciutto di Parma and Champagne are famous examples of products that are protected by their GIs, leading to high economic values.¹ Interestingly, scientific methods especially chemical methods can offer several advantages to confirm GIs, thanks to an objective nature of products, and a wealth of efficient identification methods.³⁻⁵ This has led to several investigations where chemical tools and knowledge, typically coupled with chemometrics, were employed to reveal and identify new GIs. In this regard, an overview of current chemical methods for this purpose has been classified into three groups: chromatographic techniques, spectroscopic techniques, and other miscellaneous techniques that utilized certain properties of the products of interest. The reported cases of the techniques together with their advantages and drawbacks are discussed below.

จุฬาลงกรณ์มหาวิทยาลัย
CHULALONGKORN UNIVERSITY

1.1.1 Chromatographic techniques

The purpose of these techniques is to separate and analyze numerous constituents in a mixture. Various components pass through a column unit at different rates depending on their relative affinities for mobile and stationary phases. The resulting chromatogram provides relative identities (as retention times) as long as their relative quantities of each separated compound – this can be directly exploited by chemometrics for GI purposes. It should be noted, however, that this technique still requires some detection technologies, many of which are described below in other techniques.

1.1.1.1 High-performance liquid chromatography (HPLC)

HPLC is an LC method relied on pumps to pass a pressurized liquid and a sample mixture through an adsorbent-filled column, leading to the separation of the sample components. The most common detector for HPLC is a diode-array detector (DAD). There are several reasons why HPLC-DAD has been frequently used in food analyses. This includes high reproducibility, high customizability (lots of choices for both mobile and stationary phases), and no sample destruction allowing it to be collected for further analysis. However, a main limitation is that components with no UV-visible absorption may not be detected. Yudthavorasit *et al.* discriminated gingers from five countries of origin by their chromatographic fingerprints using HPLC-DAD.⁶ Chemometric studies including Hierarchical Cluster Analysis (HCA), Principal Component Analysis (PCA) and Linear Discriminant Analysis (LDA) were conducted based on the relative peak areas of eight gingerol-related compounds. The results clearly demonstrated the relationship between the ginger profiles and their origins. Furthermore, they reported five important markers that specified to the original countries and allowed for GI authentications.

1.1.1.2 Gas chromatography (GC)

GC is one of the most universal technique used in food analysis because it gives the crucial information about volatile and semi-volatile components in samples, both of which play important roles for food qualities. This analytical technique works by separating a mixture of volatiles by their properties including polarity, molecular weight and boiling point. The volatile compounds transport in the gas phase into a GC column which are then separated and go to the detector for further analysis. Flame ionization detector (FID) is a useful general detector for organic compound detection. It has high sensitivity and low noise, but the sample is not recoverable after the analysis. Kritiotti *et al.* investigated fatty acid compositions of virgin olive oils from two olive cultivars, three altitude classes and four districts in Cyprus using GC-FID.⁷ The fatty acid composition of all samples were analyzed by chemometrics. PCA result could discriminate samples with different botanical origins but this analysis was not able to differentiate growing conditions. However, ANOVA

analysis had been studied to identify two significant markers, which are margaroleic acid for cultivar indication and palmitoleic acid for altitude and district discriminations.

1.1.2 Spectroscopic techniques

Spectroscopic techniques without any separation can sometimes be used directly to provide some useful GI information. The key advantage is the ease of sample preparation and the shorter analysis time.

1.1.2.1 Nuclear magnetic resonance (NMR) spectroscopy

NMR is based upon the measurement of absorption of electromagnetic radiation in the radio frequency region by the nuclei of atoms e.g., ^1H and ^{13}C under a strong magnetic field.⁸ This technique is regularly used for elucidating the structures of organic compounds. In addition, NMR spectrum has been applied with chemometrics to discriminate GI samples. Tomita *et al.* reported ^1H -NMR-based metabolic profiling of five apple cultivars produced in Japan and New Zealand.⁹ PCA score plot of the NMR spectra showed a clear separation of each cultivar corresponding to the differences in major sugar signals (sucrose, glucose, and fructose). Multistep PCA after removing the dominant sugar signals interestingly classified apples into two classes according to their place of production. Although NMR provides detailed information regarding to the molecular structure of samples, it seems to be too expensive for GI purposes and too complicated for general users.

1.1.2.2 Ultraviolet-visible (UV-Vis) spectroscopy

UV-Vis spectroscopy involves the determination of absorbance of a sample after being exposed to light in the UV-Vis region. It is a suitable technique for quantifying concentrations of analytes in the solution because it is simple, inexpensive, rapid and non-destructive. However, its sensitivity is chromophore-dependent. In food control, UV-Vis spectrum coupled with chemometric approaches has been utilized for GI protection. Kharbach *et al.* revealed UV fingerprints of extra virgin Argan oils from five forests in Morocco.¹⁰ PCA and partial least squares

discrimination analysis (PLSDA) of the UV profiles showed perfect discrimination from five cultivated regions and three different preparations. Compared to the fatty-acid composition experiment using gas chromatography (GC), this proposed method can provide similar predictive ability in classifying the different categories of oil samples with an easier approach.

1.1.3. Miscellaneous techniques

1.1.3.1 Sensory analysis

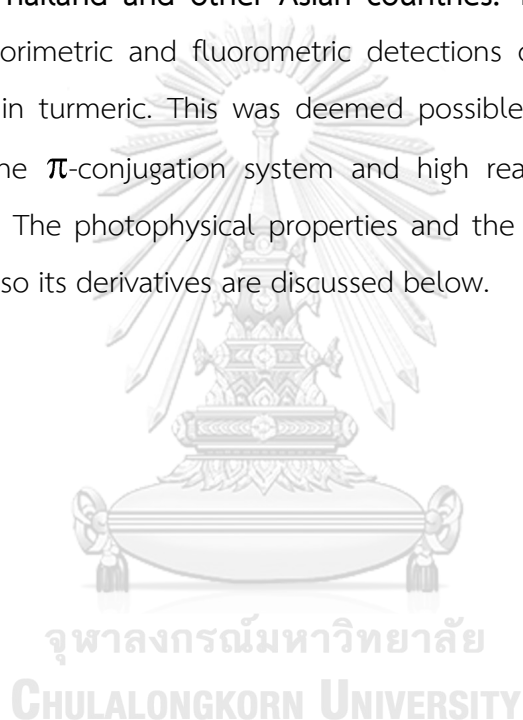
Sensory analysis is an important tool for determining food quality based on appearance, odor, flavor and texture properties. Panelists, panels of human assessors, measure the quality of products by their perceptions. The descriptive sensory analysis is combined with statistical analysis. Urvieta *et al.* presented phenolic and sensory profiles of Malbec wines from the three most important wine-making regions in Argentina.¹¹ Twelve anthocyanins and eighteen non-anthocyanins in wines from different locations were quantified using HPLC. Canonical variate analysis (CVA) based on the HPLC data effectively showed geographical classification. Moreover, PCA studies based on seven sensory attributes (red fruit, raisins, black pepper, herbaceous, tobacco, hot, and sweet) indicated a clear GI separation. This work is a showcase of the utilization of sensory data in GI studies.

1.1.3.2 Electronic nose technology

An electronic nose, a sensing array that mimics the human olfactory perception, consists of a set of semi-selective gas sensors for detecting volatile compounds. Each sensor reacts to the volatiles on contact in their specific way. The response patterns, as resistance and conductance, through the analysis time are recorded and transformed into digital data for further chemometric treatments. Gorji-Chakespari *et al.* manifested the application of the electronic nose in qualitative control of Iranian *Rosa damascena* essential oils.¹² The sensor array was designed based on seven metal oxide semiconductors to detect organic solvent vapors,

alkanes (C1-C4), alcohols and ammonia. LDA based on ten features provided the best result with three qualitative categories (low, middle, and high quality).

As evident in the aforementioned studies, chemical approaches for GI are on the basis of the power of instruments or the skill of specialists. **Instead, this research project focused on a reagent paper array as a simple, inexpensive, and portable method for the geographical discrimination of turmeric, a commonly known spice in Thailand and other Asian countries.** The device was fabricated based on the colorimetric and fluorometric detections of curcumin, which is the main component in turmeric. This was deemed possible due to its photophysical properties from the π -conjugation system and high reactivity at α,β -unsaturated carbonyl moieties. The photophysical properties and the chemical reactions of this component and also its derivatives are discussed below.



1.2 Curcumin

Turmeric (*Curcuma longa*) is an Asia- and South East Asia native plant, which belongs to the ginger family, Zingiberaceae. Similar to other plants in this family such as ginger or galangal, the rhizome of turmeric is usually used as a spice and herbal supplement. The use for traditional medicine stemmed from the fact that the major compound in turmeric, curcumin (**Figure 1**), was found to exhibit a wide range of biological activities.¹³⁻¹⁵ Although there have been some reports that caution the possible false-positive activities of curcumin,¹⁶⁻¹⁷ it is unlikely that turmeric will be abandoned. This is because it has been firmly incorporated into traditional cuisines of many countries, especially curry dishes. Therefore, the knowledge of the origins of turmeric, which may be related to its medicinal or sensory properties, is still deemed to have great economic values for the food industry.

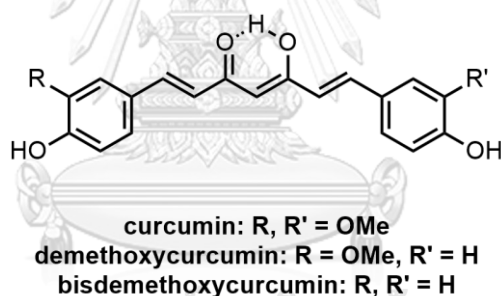


Figure 1 The chemical structures of curcumin and common derivatives

In regard to the chemistry of curcumin, this key compound usually exists as a mixture with its demethoxy derivatives (**Figure 1**).^{13, 15} As a rare naturally occurring example of α,β -unsaturated β -diketoheptanoid, curcumins possess unique structural features that, apart from their biological studies, were also investigated in other ways. For instance, its extensive π -conjugation system results in curcumin being highly colored, with a major absorption around 425 nm.¹⁸⁻¹⁹ In addition, curcumins can strongly fluoresce as a green emission (550 nm) even upon an excitation by ordinary

blacklight. This fascinating property of curcumins led to an adaptation as a safe dye for general purposes.²⁰⁻²²

Importantly, the structural feature of curcumins also allows for diverse types of chemical modifications resulting in some changes in photophysical properties. In fact, there has been reports about the uses of chemical reactions related with curcumins for other applications such as sensors. Some of these works are described below.

1.2.1 pH sensing

There are two tautomeric forms of curcumin as shown in **Figure 2**. In acidic and neutral pH, it exists mainly as a keto form. In an alkaline medium, it is deprotonated and exists as an enolate ion with concomitant red shift in UV spectrum.¹⁵

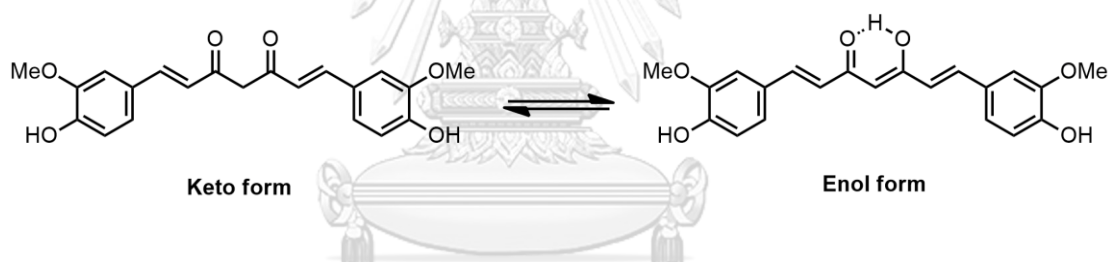


Figure 2 Tautomeric forms of curcumin.

With the pH-responsive properties, Pourreza *et al.* developed a lab-on-paper device from curcumin nanoparticles (CURNs).²³ The paper fabricated by wax-dipping method was loaded with CURNs solution and pH-solutions, respectively. The color change was captured by a digital camera and processed with Adobe Photoshop software. Mean color intensity with different pH was used as an analytical signal to quantify pH values of solution. The probe was applied to measure pH value of real water samples and the error was less than 3.3% compared to the pH meter.

1.2.2 Metal ions sensing

The most popular application is the capability of curcumins to accommodate various metal ions. Some metal-curcumin complexes showed significantly different photophysical properties, thus allowing the use of curcumins as sensors for these metal ions.

1.2.2.1 Boron sensing

The reaction of curcumin and boron with 2:1 stoichiometry in an acidic condition provides a rosocyanine complex (**Figure 3**). It is bright red in the solution and can be used for boron detection. Lawrence *et al.* reported an effective TLC straining method based on the formation of the rosocyanine complex.²⁴ By dipping a developed TLC in the curcumin solution and simply drying with a heat gun, leftover phenyl boronic acid in Suzuki coupling was monitored as an orange spot. This method can be applied to other boronic acids; however, it did not work well in strongly basic condition due to the brown color of deprotonated curcumin.

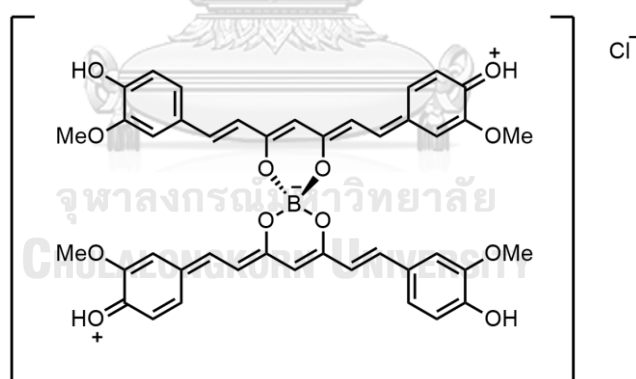


Figure 3 Chemical structure of rosocyanine complex.

1.2.2.2 Iron sensing

Bhat *et al.* revealed the utility of turmeric extract as a colorimetric detection for Fe^{2+} ion.²⁵ The bathochromic shift and fluorescence quenching were attributed to the formation of 1:2 curcumin-metal complex which resulted in intramolecular

charge transfer transition. The binding mechanism (Figure 4) has been confirmed by UV-Vis and fluorescence titrations.

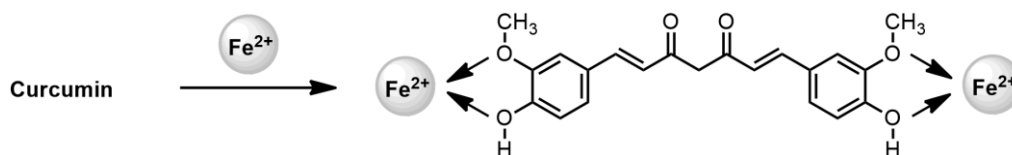


Figure 4 Proposed mechanism for the Fe^{2+} ions binding to curcumin.

1.2.2.3 Lead sensing

Raj *et al.* fabricated curcumin loaded cellulose acetate nanofiber by electrospinning method.²⁶ The strip selectively detected Pb^{2+} ion and caused a color change from yellow to orange. Quantitative detection was performed on Pb^{2+} ion and showed a detection limit of 20 μM by naked eyes. Notably, the optimum pH of this sensor was in the range of 5 to 11, and it did not show any visible color change at pH 3-4.

Regarding the aforementioned studies, curcumin can react with various reagents both in solution and on the cellulose surface. The color changes can be easily monitored by naked eyes or fluorescence. This occurs quickly and requires mild conditions (no heat or catalysts needed) which is amenable to the paper-based chemical arrays. **This work focused on the observation of the color changing of curcumin and its derivatives in turmeric samples that are perturbed by other components depending on each origin.** To fully maximize the usefulness of the data, however, chemometric analysis can further maximize the use of these discrimination data.

1.3 Chemometrics

Most GI studies using chemical methods created a large set of data. This requires a systematic tool to operate and differentiate data among samples. Chemometrics is one of the best tools that applies mathematical and statistical methods to improve chemical measurement and to extract useful information from chemical measurement data.²⁷ The chemometric approaches can greatly improve the clarity of information obtained from complex chromatographic or spectroscopic profiles. The pattern recognition can be divided into two categories of as follows.

1.3.1 Unsupervised pattern recognition

This type of pattern recognition is the multivariate data analysis that is most popular for data visualization in order to observe the relationship between samples and variables with no predetermined class. This analytical tool allows samples to be allocated in the clusters based on their relations.

1.3.1.1 Cluster Analysis (CA)

CA is a grouping technique to arrange data objects into a number of homogeneous subgroups called clusters based on the observed values of several variables for each individual. The most popular type of CA is Hierarchical Cluster Analysis (HCA), which allows for better understanding of the relations among the sample objects shown as a hierarchy of clusters. Beginning with an own cluster of each object, the two most similar clusters are connected into a new larger cluster. With this repeating process, all objects will be end up with one big cluster. The whole cluster of all sample objects in HCA are ordered in one-dimensional sequence called a hierarchical tree diagram or dendrogram (**Figure 5**). The distance pattern reveals sample profiles through simple interpretation. The smallest distance indicates the highest degree of relationship.

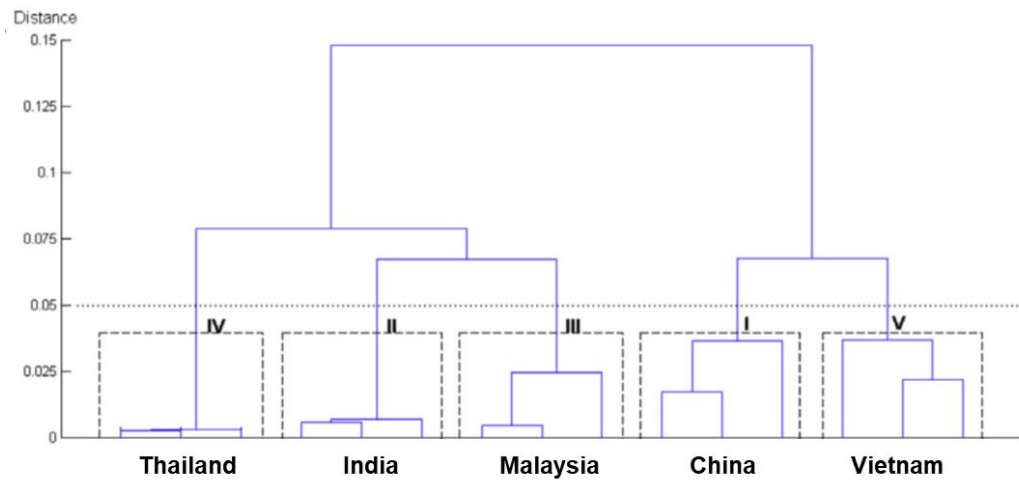


Figure 5 An example of HCA dendrogram.⁶

1.3.1.2 Principal Component Analysis (PCA)

PCA is a well-known data analysis technique to monitor the outline of all data in multivariate analyses. This works by reducing a large number of variables in multidimensional data sets to a lower number of dimensions called principal components (PCs). From PC score plot (**Figure 6**), PC1 is considered as the greatest variance among all possible linear combinations. PC2, orthogonal to PC1, is accounted for the second greatest variance. Other PCs indicate smaller variability of data. Notably, each PCs are always uncorrelated and the closer of the summation of percentage described by PCs to 100% refers to a more faithfulness of the model of data visualization. Samples that are closed to each other will have scores that cluster together. In contrast, different samples are shown farther apart in the PC space.

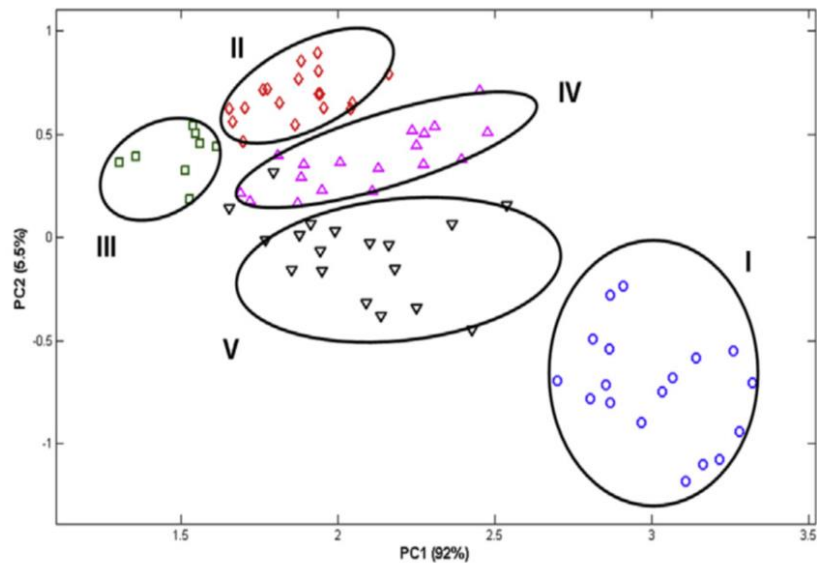


Figure 6 An example of two-dimensional PC score plot.⁶

1.3.2 Supervised pattern recognition

This developed pattern recognition is a conventional method to classify a large number of data. This statistical process attempts to create a model to predict the class of an unknown sample.

1.3.2.1 Linear Discriminant Analysis (LDA)

LDA is a well-known method that provides a mathematical model for classifying and identifying sample according to their class. It has been used for class prediction purposes by assigning linear classifiers or boundaries on the data set using linear discriminant functions in order to define the direction that maximizes the separation of all determined classes. The classification performance can be evaluated by leave-one-out cross validation. This is performed by assigning one sample as a test set with others as a training set. The validation starts with creating a model from the training set, followed by predicting the test set. After repeating the procedure for all samples, the performance of the developed classifier is indicated by a percentage of predictive ability.

LDA is closely related to PCA in that both pattern recognitions produce a number of linear functions for dimensionality reduction. However, the major difference between LDA and PCA is that LDA creates linear discriminants that maximize the separation between the given classes without any change of data location, while PCA ignores the class labels. It focuses on the reduction of variance into fewer principal components that maximize the variance in a dataset with changing of the shape and location.



1.4 Purpose of this study

In this study, the photophysical changes of curcumins upon reacting with various reagents were exploited as a means to differentiate and identify sources of turmeric. The key hypothesis was that subtle differences in chemical components in each turmeric extract may affect the kinetics and thermodynamics of each reaction in different ways, depending on specific compositions of each extract. This can then be used as a differentiation method to identify turmeric sources. In order to make it even simpler, we aimed to omit the use of sophisticated instruments like various spectrophotometers. Instead, only common household tools including a document scanner, a digital camera, and a commercial blacklight were utilized to capture image data from chemical reactions performed on paper arrays. After some chemometric treatment, it was found that these simple tools were effective in identifying the sources of turmeric. Given its simple platform, this approach may also be a viable tool for simple geographical indications of other plants having a variety of chromophores.

CHAPTER II

EXPERIMENTAL SECTION

2.1 Materials and chemicals

Chemical reagents and solvents were purchased from Sigma-Aldrich, Fluka, Carlo Erba, Chem-Impex Ltd., May & Baker Ltd., Baker Analyzed, Merck and RCI Labscan (Thailand). All chemicals are listed below:

- Acetonitrile (CH_3CN)
- Copper (II) sulfate ($\text{CuSO}_4 \cdot 5\text{H}_2\text{O}$)
- Curcumin analytical standard (98% purity)
- Dichloromethane (CH_2Cl_2)
- 2,4-dinitrophenylhydrazine (DNP)
- Formic acid (HCOOH)
- Hydrochloric acid (HCl)
- Iron (II) sulfate ($\text{FeSO}_4 \cdot 7\text{H}_2\text{O}$)
- Lead (II) nitrate ($\text{Pb}(\text{NO}_3)_2$)
- Methanol (CH_3OH)
- Nickle (II) sulfate ($\text{NiSO}_4 \cdot 6\text{H}_2\text{O}$)
- Sodium borate ($\text{Na}_2\text{B}_4\text{O}_7$)
- Sodium dihydrogenphosphate ($\text{NaH}_2\text{PO}_4 \cdot \text{H}_2\text{O}$)
- Sodium hydrogenphosphate ($\text{Na}_2\text{HPO}_4 \cdot 2\text{H}_2\text{O}$)
- Sodium hydroxide (NaOH)
- Sulfuric acid (H_2SO_4)
- Vanillin

Fresh turmeric rhizomes (*Curcuma longa*) from four different sources, and turmeric powders from six different sources were obtained and used in this study. Fresh turmeric samples were purchased from local markets. Samples originated from outside Thailand were purchased online. The origins of these samples can be found in **Table 1**.

Table 1 The origins of turmeric samples used in this study.

Sample	Source Location	Type
Cur1	Chumphon, Thailand	Fresh turmeric
Cur2	Bangkok, Thailand	Fresh turmeric
Cur3	Singapore	Fresh turmeric
Cur4	China	Fresh turmeric
Cur5	Thailand	Turmeric powder
Cur6	Thailand	Turmeric powder
Cur7	Vietnam	Turmeric powder
Cur8	India	Turmeric powder
Cur9	Myanmar	Turmeric powder
Cur10	China	Turmeric powder
Cur11	USA	Curcumin standard, 98%

2.2 Extraction procedure

One gram of oven-dried (72 hours at 50 °C), small cubic turmeric (or dry powder for powder samples) was added with methanol (5 mL), and the resulting mixture was heat at 65 °C for 4 hours using AccuBlock™ digital dry bath heater (Labnet). Thereafter, methanol solution was removed, and the crude solid was added with dichloromethane (5 mL), followed by brief vortexing. The dichloromethane portion was then combined with the methanol portion, and the mixture was subject to rotary evaporation to remove all solvents. Dry crude was re-added with methanol to create a stock solution at 5 mg/mL, with further dilutions depending on applications: HPLC-DAD = 1 mg/mL, LC-MS = 0.25 mg/mL, and reactions on paper arrays = 1 mg/mL.

Curcumin analytical standard (98% purity) was diluted in methanol to create a stock solution at 1mg/mL, with further dilutions depending on applications: HPLC-DAD = 0.2 mg/mL, LC-MS = 0.05 mg/mL, and reactions on paper arrays = 0.2 mg/mL.

2.3 Determination of main components in turmeric extracts

2.3.1 High-performance liquid chromatography (HPLC)

All HPLC experiments with a photodiode array detector (DAD) were performed with the following parameters. Model: Ultimate 3000, Thermo Fisher Scientific; column: VertiSep™ UPS C18 column, 4.6 x 50 mm, 3 μm; injection volume: 10 μL; mobile phases: solvent A = 0.1% aqueous formic acid, solvent B = 0.1% formic acid in acetonitrile; flow rate: 0.5 mL/min; time program: 30% B for 2 minutes, linear gradient to 90% B over 18 minutes, held at 90% B for 10 minutes, and a final decrease to 30% B.

DNP reaction condition with turmeric samples. DNP stock solution (0.2 M) described below (**Table 2**) was further diluted with methanol to 8 mM. Thereafter, 200 μL of the stock solution (5 mg/mL) from turmeric extract was added with 300 μL of methanol and 500 μL of 8 mM DNP solution. The final concentrations were 1 mg/mL for crude turmeric, and 4 mM for DNP. This solution was briefly vortexed and then incubated for 3 hours. The resulting solution was subject to HPLC analysis after filtration with 0.22-μm nylon syringe filter.

2.3.2 Liquid chromatography – tandem mass spectrometry (LC-MS)

All LC-MS experiments with a quadrupole time-of-flight (QTOF) detector were performed with the following parameters. UHPLC model: 1290 Infinity II, Agilent; mass spectrometer: SciEx X500R QTOF MS.; column: VertiSep™ UPS C18 column, 4.6 x 50 mm, 3 μm; injection volume: 10 μL; mobile phases: solvent A = 0.1% aqueous formic acid, solvent B = 0.1% formic acid in acetonitrile; flow rate: 0.5 mL/min; time program: the same as the HPLC-DAD experiments.

MS parameters: mass range = 80–800 m/z , positive mode; ion source gas 1 = 40 psi; ion source gas 2 = 50 psi; source temperature = 500 °C; spray voltage = 5500 V; declustering potential (DP) = 50 V; collision energy (CE) = 10 V. MS/MS parameters: mass range = 80–800 m/z , DP = 80 V; CE = 35 ± 15 V. SciEx OS software was used to process all data.

DNP reaction condition with turmeric samples. The protocol was exactly the same as the one for HPLC-DAD analyses, but the final solution after 3-hour incubation was further diluted at 1:4 with methanol before analysis.



2.4 Fabrication of paper arrays

A 20 x 20 cm 1Chr Whatman chromatography paper was patterned as hydrophilic circular shapes (0.48 cm diameter) by wax printing with a Xerox ColorQube 8580 printer (**Figure 7**). The sheet was then cut into desired portions and heated at 185 °C for 30 seconds. Thereafter, each sheet was attached with a transparent tape on the back side.

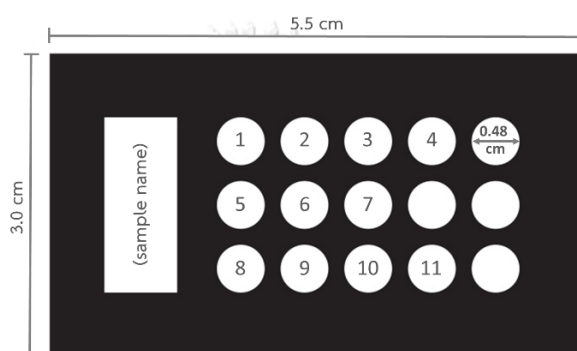


Figure 7 The pattern of the arrays used in this study.

The reagents used in this study were prepared as in **Table 2**. Each reagent (5 μL) was dropped into each well and air-dried for 1 hour. This was followed by dropping 5 μL of turmeric solution into the arrays with 1-hour incubation.

After the incubation step, a HP Deskjet Ink Advantage 2515 scanner (600 dpi) was used to obtain images under white light. This was then followed by obtaining images under 365-nm UV light using a Sony ILCE-5100 camera (settings: ISO 200, shutter speed at 1/4 s, and F value at 14) and a transilluminator (Vilber Lourmat 8W dual wavelength (312 & 365 nm)) with a handmade cardboard box to fix an image distance at 22.5 cm. These digital images were converted into red, green, blue (RGB) values for chemometric experiments and mean color intensities for LOD experiments using ImageJ processing software. An area of selection was set as a circular region with an average size of 1800 square pixels.

Table 2 All reagents used in the paper arrays.

Well	Reagent	Concentration (mM)	Reagent preparation
1	H ₂ O	-	Milli-Q water
2	pH 2	100	Phosphate buffer at pH 2 in Milli-Q water
3	pH 7	100	Phosphate buffer at pH 7 in Milli-Q water
4	pH 12	100	Phosphate buffer at pH 12 in Milli-Q water
5	DNP	4	<p>Stock solution (0.2 M): 2 g of DNP was added into 10% H₂SO₄ in methanol (40 mL). The solution was warmed at 50 °C for 1 hour and then added with 10 mL of water. The solution was kept at rt for 2 hour and filtered insoluble solid out.</p> <p>The stock solution was diluted in Milli-Q water at 1:50 dilution.</p>
6	Vanillin	6.6	<p>Stock solution (66 mM): 10 mg of vanillin was dissolved in 70% aqueous H₂SO₄ (1 mL).</p> <p>The stock solution was diluted in Milli-Q water at 1:10 dilution.</p>
7	H ₃ BO ₃	5	<p>Stock solution (50 mM): 6.5 mg of Na₂B₄O₇ was dissolved in 30% aqueous H₂SO₄ (1 mL).</p> <p>The stock solution was diluted in Milli-Q water at 1:10 dilution.</p>

Table 2 (continued).

Well	Reagent	Concentration (mM)	Reagent preparation
8	Cu^{2+}	1	Stock solution (50 mM): 125 mg of $\text{CuSO}_4 \cdot 5\text{H}_2\text{O}$ was dissolved in 10-mL Milli-Q water. The stock solution was diluted in Milli-Q water at 1:50 dilution
9	Fe^{2+}	1	Stock solution (50 mM): 140 mg of $\text{FeSO}_4 \cdot 7\text{H}_2\text{O}$ was dissolved in 10-mL Milli-Q water. The stock solution was diluted in Milli-Q water at 1:50 dilution.
10	Ni^{2+}	10	Stock solution (50 mM): 130 mg of $\text{NiSO}_4 \cdot 6\text{H}_2\text{O}$ was dissolved in 10-mL Milli-Q water. The stock solution was diluted in Milli-Q water at 1:5 dilution.
11	Pb^{2+}	10	Stock solution (50 mM): 165 mg of $\text{Pb}(\text{NO}_3)_2$ was dissolved in 10-mL Milli-Q water. The stock solution was diluted in Milli-Q water at 1:5 dilution.

2.5 Chemometrics

A multidimensional data set was created using RGB numerical values on both visualization modes (white and UV lights) of each reagent spot. The relation of sample was visualized by Principal Component Analysis (PCA) using MATLAB version 9.4 (R2018a) software.

The classification was performed using Linear Discrimination Analysis (LDA) with leave one out cross validation approach. All calculation software was in-house generated based on MATLAB version 9.4 (R2018a) platform. LDA computation involves two main parts.

First, all combinations of factors and variables were calculated based on binary numeral system. This involves all possible combination of n elements (reagents) equal to $2^n - 1$ (the combination of all zeros was ignored). As our dataset contains 11 elements, it will involve $2^{11} - 1 = 2047$ combinations. Notably, one reagent always contains 6 data (3 RGB numerical data with 2 visualization modes).

Second, the dataset with only selected elements was used to for further calculation based on LDA approach. Briefly, the distance between samples to the class centroid is weighted according to the overall variance of each variable/element. The class of sample is determined as the class that provides the smallest distance to the sample.

CHAPTER III

RESULTS AND DISCUSSION

3.1 Determination of main components in turmeric extracts

In order to better understand the nature of the extracts, the investigation started with some characterizations of the crudes before any chemical reaction. High-performance liquid chromatography (HPLC) experiments were conducted. As curcuminoids are known to absorb strongly at around 426 nm, this wavelength was used for curcumin quantification. A Calibration curve of the curcumin standard at a retention time of 13.4 minute is illustrated in **Figure 8**. The concentrations of curcumin in crude extracts (1 mg/mL) calculated from this calibration curve are shown in **Table 3**. Curcumin contents found in all samples were below 0.25 mg/mL except two samples (**Cur3** from Singapore and **Cur8** from India). The highest amount of curcumin was found in **Cur3** at 0.370 mg/mL, and the lowest amount was found in **Cur10** from China at 0.003 mg/mL.

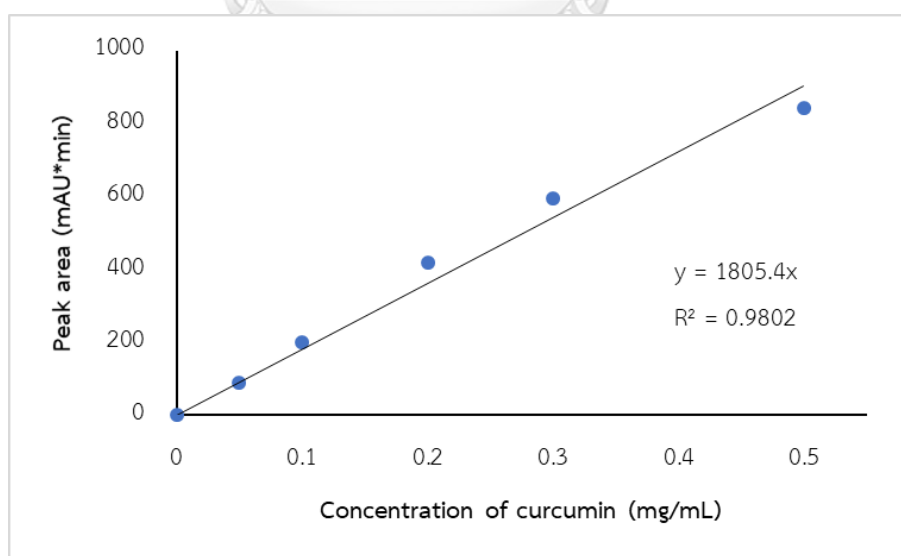


Figure 8 Calibration plot of peak areas of curcumin standard from HPLC experiment (at 426 nm, 3 replicates).

Table 3 Curcumin concentrations in methanol extracts of turmeric from different sources (at 426 nm, 3 replicates).

Sample	Peak area at 426 nm (mAU*min)	Curcumin concentration (mg/ml)
Cur1	312.92 ± 23.26	0.173 ± 0.013
Cur2	369.46 ± 7.59	0.205 ± 0.004
Cur3	668.42 ± 21.59	0.370 ± 0.012
Cur4	205.29 ± 12.63	0.114 ± 0.007
Cur5	323.52 ± 17.52	0.179 ± 0.010
Cur6	279.69 ± 25.78	0.155 ± 0.014
Cur7	108.88 ± 7.18	0.060 ± 0.004
Cur8	476.35 ± 18.30	0.264 ± 0.010
Cur9	32.02 ± 2.00	0.018 ± 0.001
Cur10	5.70 ± 0.29	0.003 ± 0.000

Furthermore, the wavelength of 250 nm was also selected to reveal more peaks of other components and curcuminoids which can still be seen at this wavelength. In all cases, curcumin and demethoxy derivatives were clearly found at 12.8, 13.1, and 13.4 minutes, respectively (**Table 4**). Also, the identities of these compounds were both verified from a comparison with an authentic standard, and from liquid chromatography – tandem mass spectrometry (LC-MS) experiments (**Table 5**), which accurately revealed the highly accurate m/z values of all curcumin derivatives at these same positions. Interestingly, some other components absorbing at 250 nm were also visible in this exemplary extract, e.g., at 17.8, 19.6 and 20.6 minutes (**Table 4**). MS data (molecular masses and certain MS/MS fragmentation patterns), along with comparisons with previous studies,²⁸⁻²⁹ suggested that most of these compounds are known sesquiterpenes typically found in turmeric such as turmerone species (**Table 5**).

Table 4 HPLC chromatograms of methanol extracts from different sources of turmeric (at 250 nm).

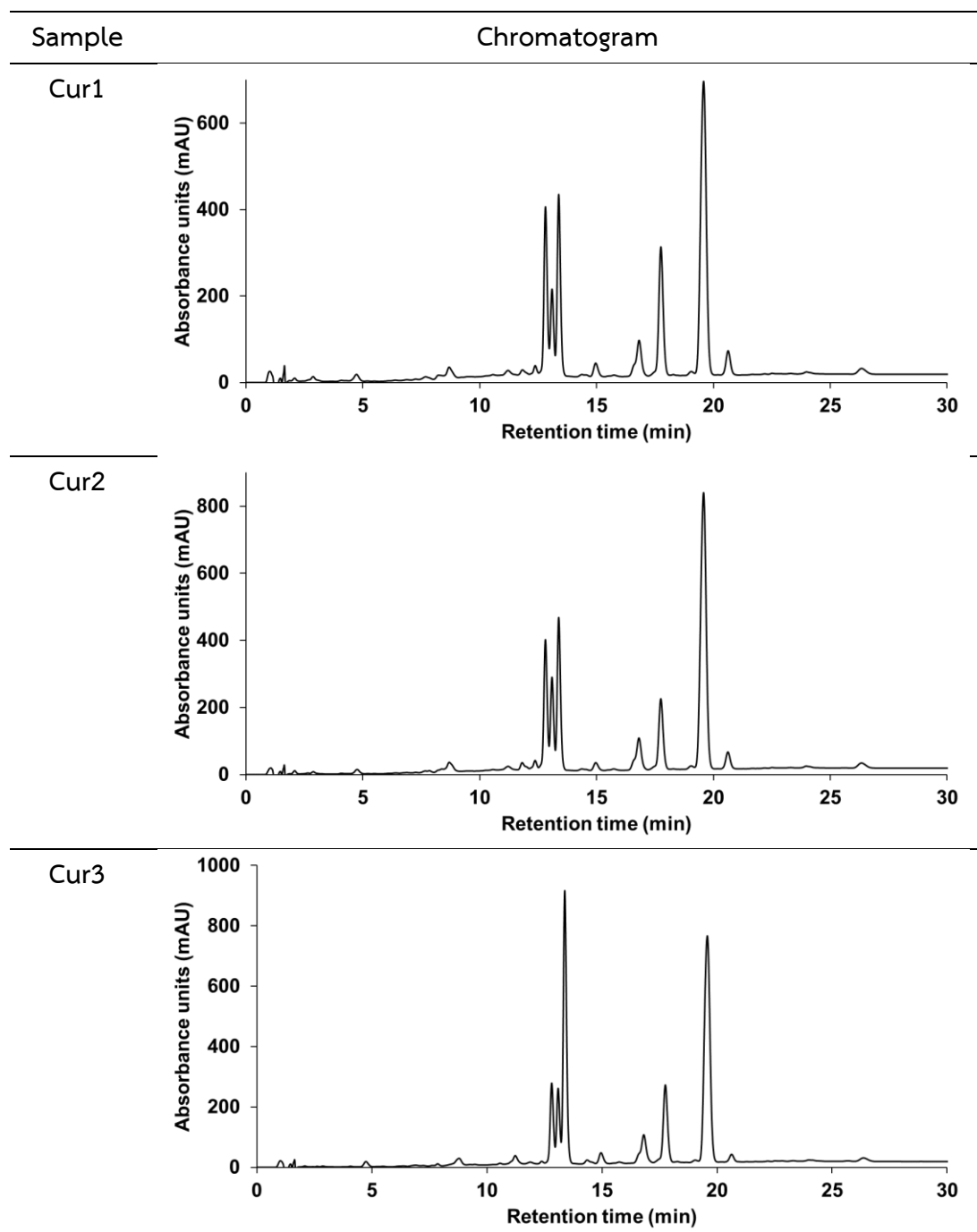


Table 4 (continued).

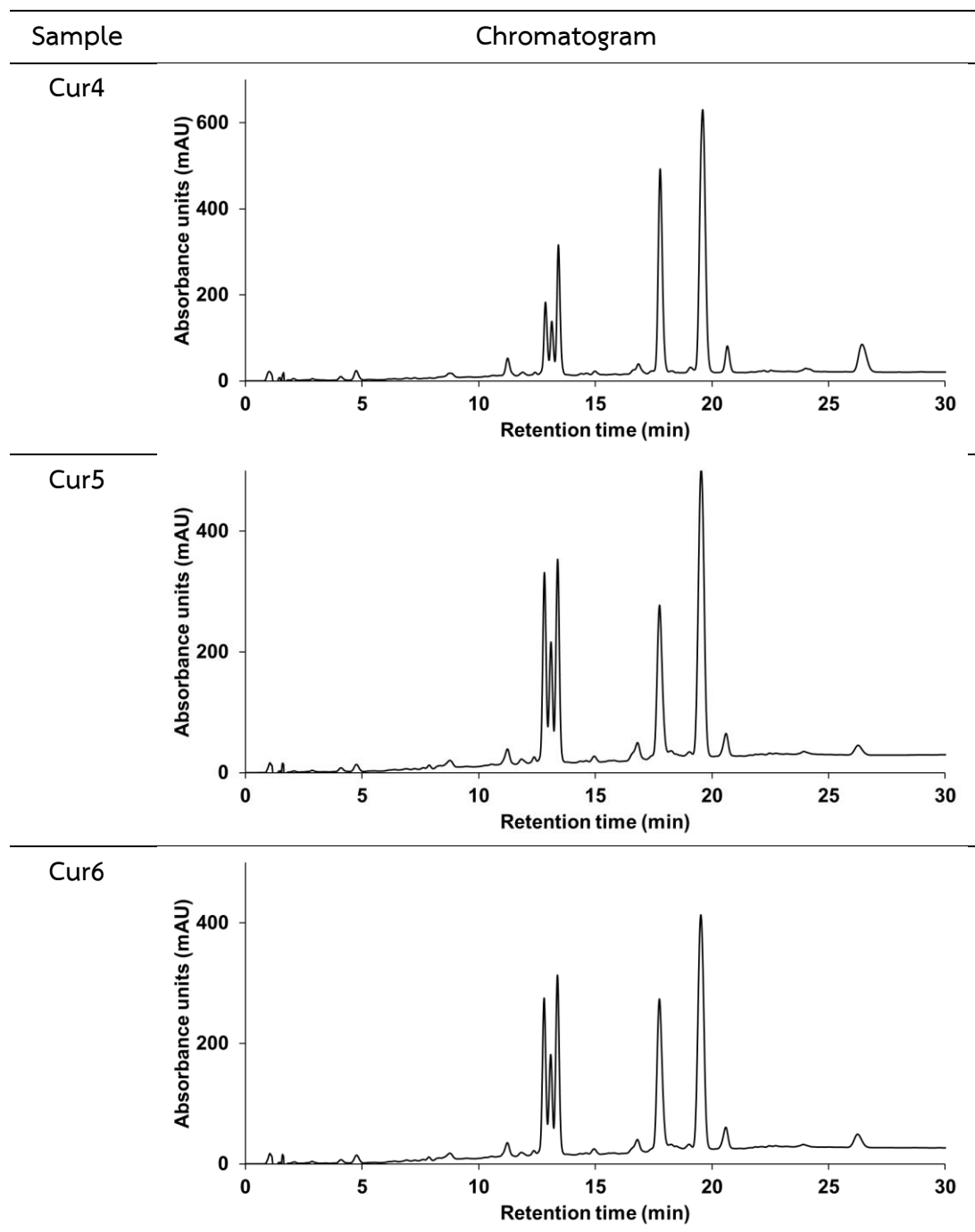


Table 4 (continued).

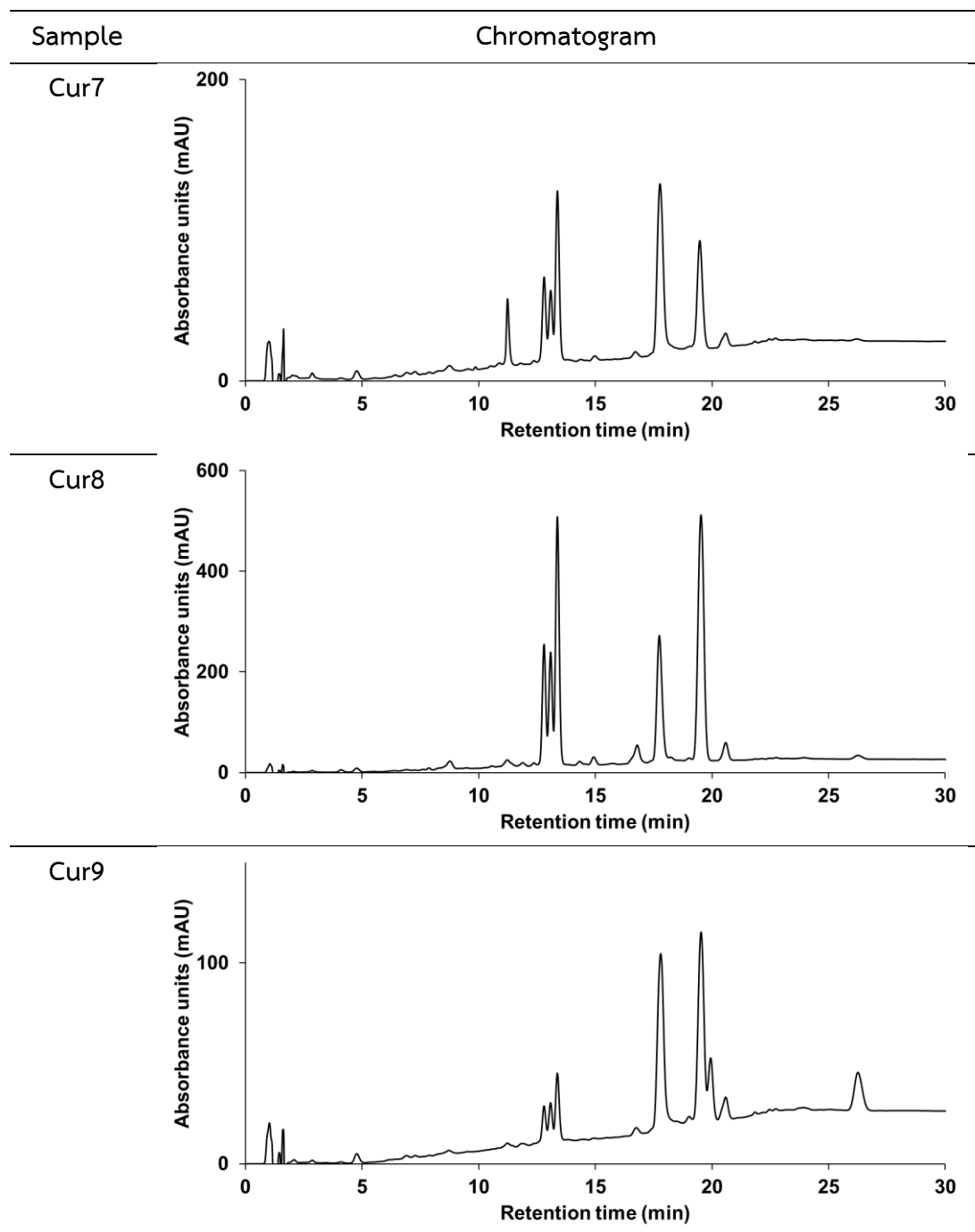


Table 4 (continued).

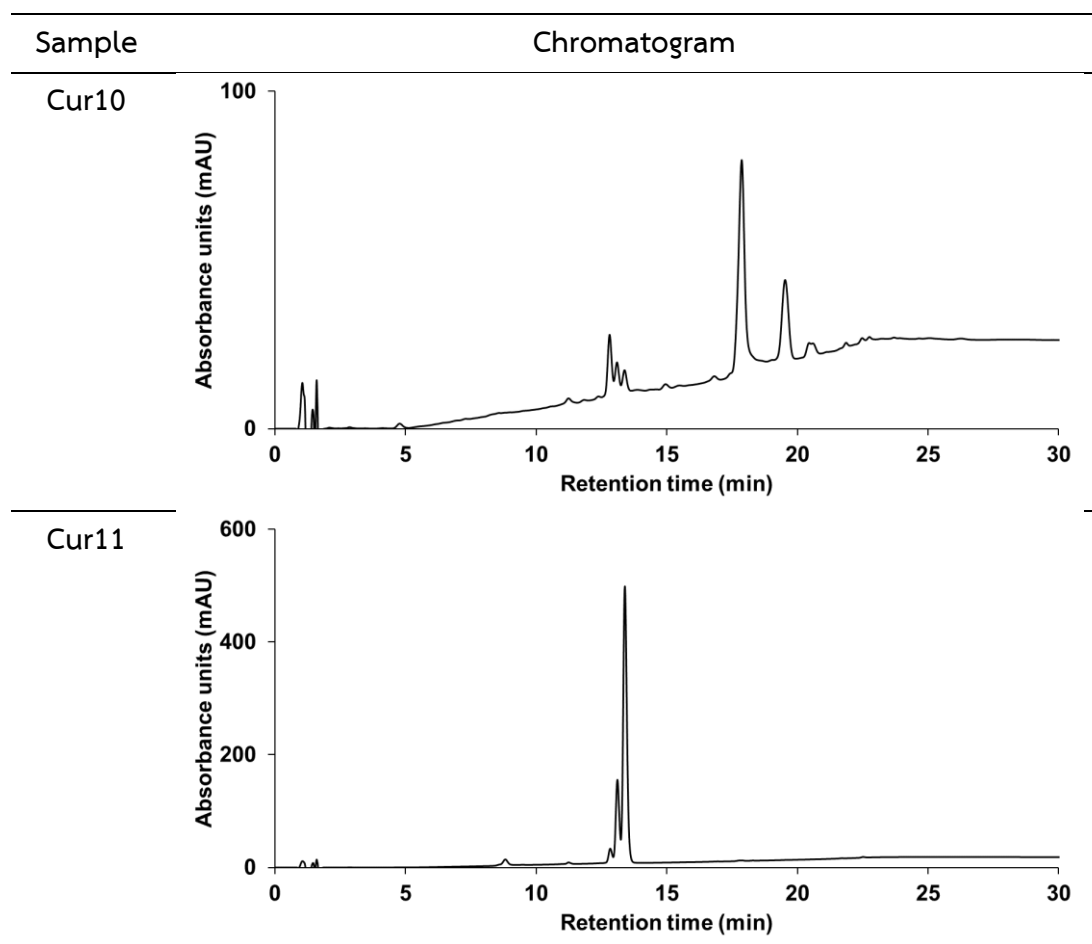


Table 5 Peak identifications of a methanol extract from Cur2.

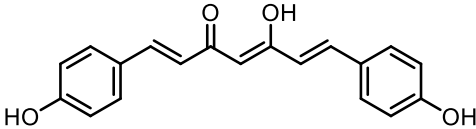
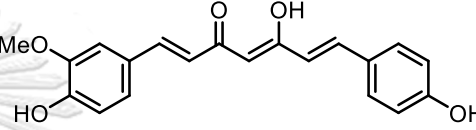
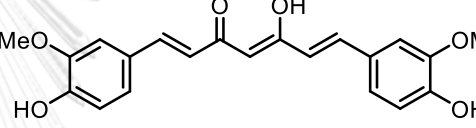
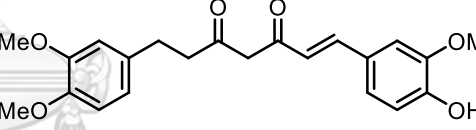
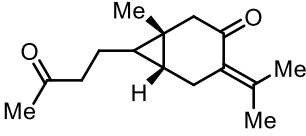
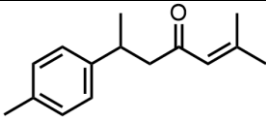
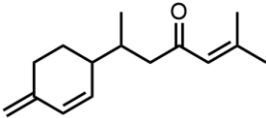
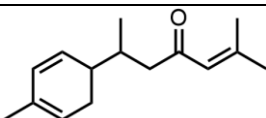
Entry	RT (min)	Found at <i>m/z</i>	Proposed Molecular Formula	Proposed structure
1	12.81	309.1120	C ₁₉ H ₁₆ O ₄	 <p>bisdemethoxycurcumin</p>
2	13.09	339.1225	C ₂₀ H ₁₈ O ₅	 <p>demethoxycurcumin</p>
3	13.38	369.1329	C ₂₁ H ₂₀ O ₆	 <p>curcumin</p>
4	14.97	385.1649	C ₂₂ H ₂₄ O ₆	 <p>compound A (or its regioisomers on -OMe groups or the double bond)</p>
5	16.83	235.1691	C ₁₅ H ₂₂ O ₂	 <p>curcumenone</p>

Table 5 (continued).

Entry	RT (min)	Found at m/z	Proposed Molecular Formula	Proposed structure
6	17.77	217.1585	$C_{15}H_{20}O$	 <i>ar</i> -turmerone
7	19.57	219.1736	$C_{15}H_{22}O$	 β -turmerone
8	20.62	219.1737	$C_{15}H_{22}O$	 α -turmerone

The bar graph compares the relative abundance of the main components in turmeric samples (Figure 9). It can be clearly seen that β -turmerone is the major compound found in all samples except in Cur10. Importantly, both the amounts of total curcumins and non-curcumin components obviously differ from one source to another. In fact, these differences were confirmed to be sufficient for differentiating sources of turmeric in a previous study using HPLC.³⁰ In our case, we hypothesized that these differences in chemical contents also affect the reactivity of curcuminoids in reacting with various reagents, which in turn may be used as another means of differentiation.

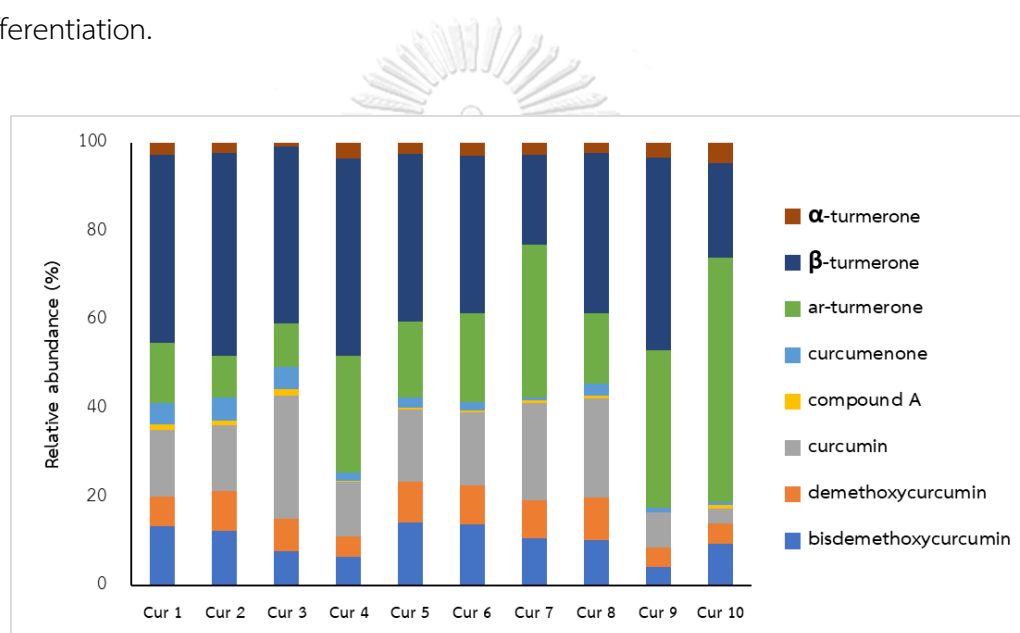


Figure 9 Relative abundance of main components in turmeric extracts (at 250 nm).

To test this hypothesis, we proceeded to perform imine formation reaction with DNP. As shown in **Figure 10A**, several new peaks appeared. Although identifying all newly formed species is not relevant to our main goal, some peaks were characterized by accurate MS (**Table 6**). For instance, apart from the remaining DNP and curcumin derivatives, hydrazone derivatives of several previously detected curcumins could be seen, e.g., signals at 16.6 and 18.0 minutes (entries 11–16 in **Table 6**). Apart from these hydrazones, further condensation and tautomerization also resulted in putative cyclic products (denoted “condensed hydrazone”) – this could be unambiguously confirmed by MS at 14.1, 14.4, and 14.6 minutes for **Cur2** sample. The proposed reaction mechanism can be found in **Figure 11**. As a comparison, a similar reaction was conducted with the **Cur3** sample, which clearly showed different peak patterns (**Figure 10B**). This finding implies that our hypothesis is likely correct, and an array of sufficient numbers of chemical reactions may allow indications of turmeric sources.

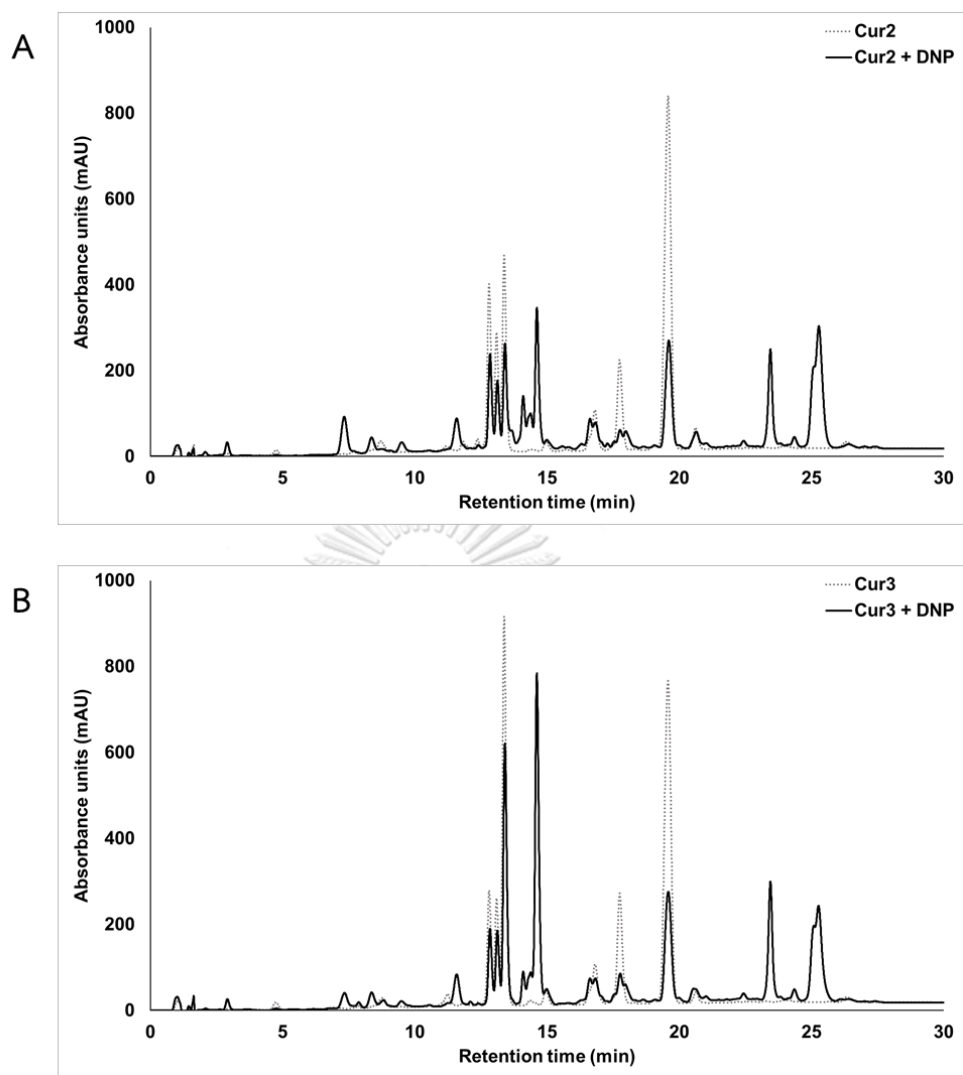


Figure 10 HPLC chromatograms of methanol extracts from (A) Cur2 and (B) Cur3 before and after reacting with DNP (at 250 nm).

Table 6 Peak identifications of a methanol extract from *Cur2* after reacting with DNP.


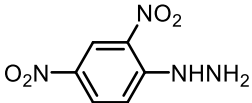
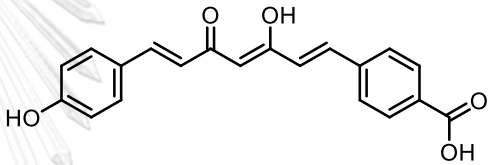
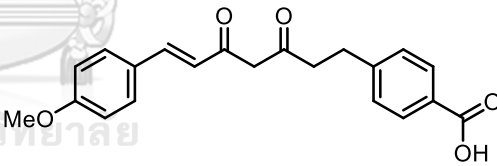
Entry	RT (min)	Found at <i>m/z</i>	Proposed Molecular Formula	Proposed structure
1	7.33	139.0501	C ₆ H ₆ N ₂ O ₂	 p-nitroaniline
2	8.35	199.0460	C ₆ H ₆ N ₄ O ₄	 DNP
3	9.51	337.1070	C ₂₀ H ₁₆ O ₅	 compound B (or other structural isomers)
4	11.58	353.1382	C ₂₁ H ₂₀ O ₅	 compound C (or other structural isomers)
5	12.85	309.1118	C ₁₉ H ₁₆ O ₄	bisdemethoxycurcumin
6	13.13	339.1225	C ₂₀ H ₁₈ O ₅	demethoxycurcumin
7	13.41	369.1330	C ₂₁ H ₂₀ O ₆	curcumin

Table 6 (continued).

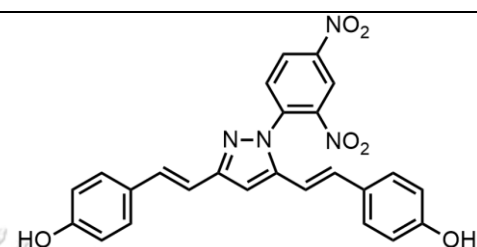
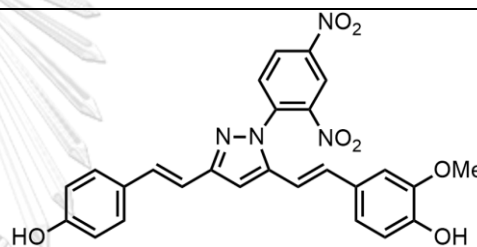
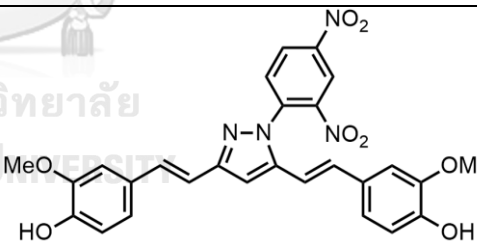
Entry	RT (min)	Found at m/z	Proposed Molecular Formula	Proposed structure
8	14.10	471.1295	$C_{25}H_{18}N_4O_6$	 <p>The condensed hydrazone product of bisdemethoxycurcumin</p>
9	14.38	501.1403	$C_{26}H_{20}N_4O_7$	 <p>The condensed hydrazone product of demethoxycurcumin</p>
10	14.62	531.1505	$C_{27}H_{22}N_4O_8$	 <p>The condensed hydrazone product of curcumin</p>

Table 6 (continued).

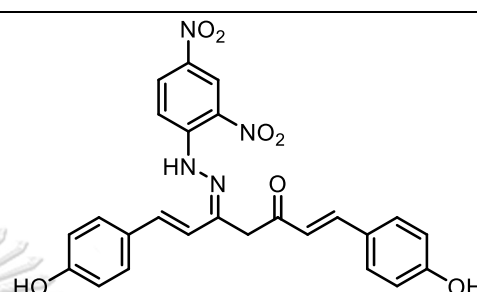
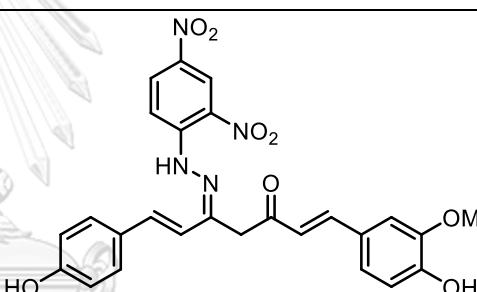
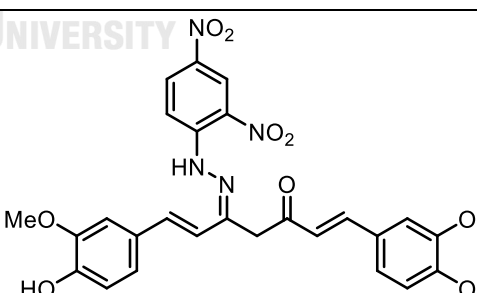
Entry	RT (min)	Found at m/z	Proposed Molecular Formula	Proposed structure
11	16.63	489.1409	$C_{25}H_{20}N_4O_7$	 <p>The hydrazone product of bisdemethoxycurcumin (keto)</p>
12	16.63	519.1514	$C_{26}H_{22}N_4O_8$	 <p>The hydrazone product of demethoxycurcumin (keto)</p>
13	16.63	549.1611	$C_{27}H_{24}N_4O_9$	 <p>The hydrazone product of curcumin (keto)</p>

Table 6 (continued).

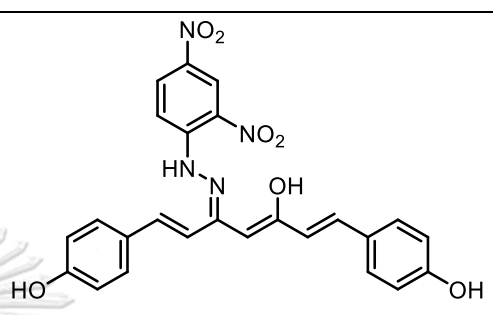
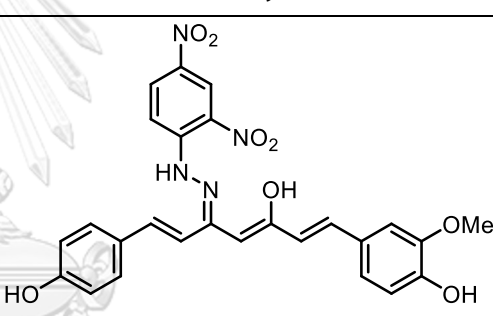
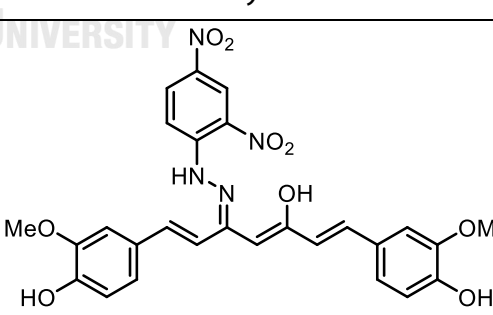
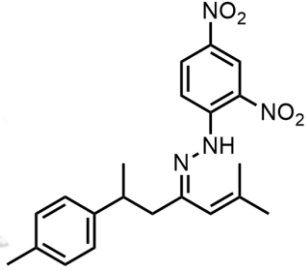
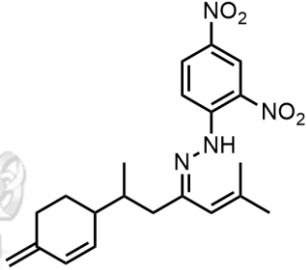
Entry	RT (min)	Found at m/z	Proposed Molecular Formula	Proposed structure
14	17.98	489.1403	$C_{25}H_{20}N_4O_7$	 <p>The hydrazone product of bisdemethoxycurcumin</p>
15	17.98	519.1512	$C_{26}H_{22}N_4O_8$	 <p>The hydrazone product of demethoxycurcumin</p>
16	17.98	549.1612	$C_{27}H_{24}N_4O_9$	 <p>The hydrazone product of curcumin</p>
17	19.61	219.1740	$C_{15}H_{22}O$	β -turmerone
18	20.65	219.1737	$C_{15}H_{22}O$	α -turmerone

Table 6 (continued).

Entry	RT (min)	Found at <i>m/z</i>	Proposed Molecular Formula	Proposed structure
19	22.44	415.1977	C ₂₁ H ₂₆ N ₄ O ₅	The hydrazone product of curcumenone
20	23.45	397.1858	C ₂₁ H ₂₄ N ₄ O ₄	 <p>The hydrazone product of <i>ar</i>-turmerone</p>
21	25.28	399.2018	C ₂₁ H ₂₆ N ₄ O ₄	 <p>The hydrazone product of β-turmerone</p>

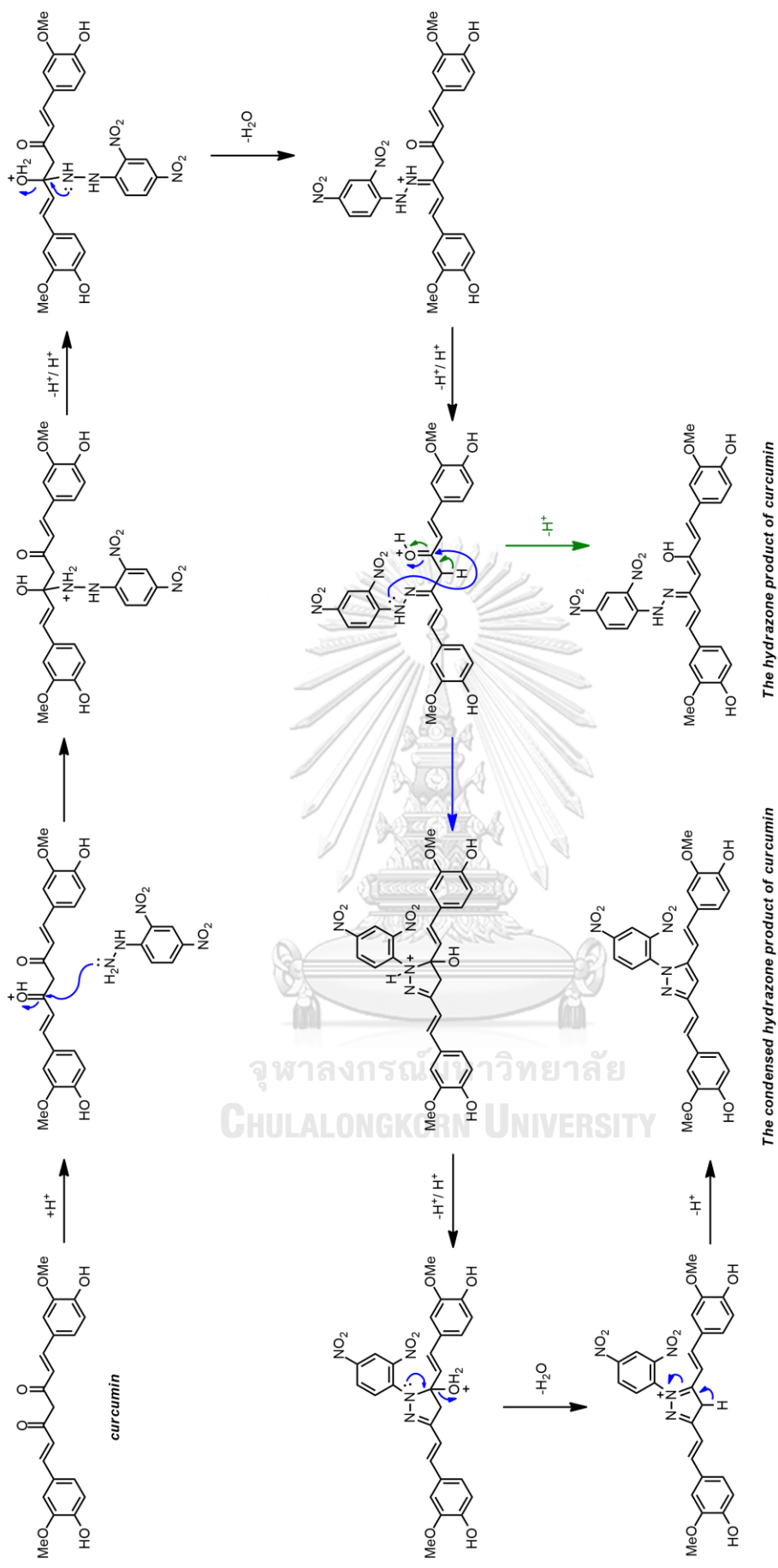


Figure 11 Proposed mechanism for the hydrazone formation and subsequent condensation of curcumin.

3.2 Chemical detection on paper arrays

Encouraged by the aforementioned results, chemical arrays were then fabricated. This was performed by wax-printing a simple circular pattern on laboratory papers. Each circular area was then used to drop a variety of chemical reagents, which were selected based on known evidences of aforementioned spectroscopic changes^{25-26, 31-38} and in-house confirmation experiments. Lastly, a turmeric extract solution to be investigated was dropped on each reaction well for testing, followed by 1-hour incubation at ambient environment. As shown in **Figure 12A**, some interactions and reactions clearly changed the color profile of the original turmeric solutions. Prominent examples include the red color from basic condition (pH 12),²³ the bright red rosocyanine produced from a well-known complexation with H_3BO_3 (produced from $\text{B}_4\text{O}_7^{2-}$ and H_2SO_4)^{33, 36} and orange-brown color generated from the complexes between curcumin with Fe^{2+} .²⁵ Furthermore, the observation of fluorescence also revealed extra information as some reagents could reduce the fluorescence intensity from curcumins including Cu^{2+} ,³⁹ Fe^{2+} , and DNP (**Figure 12B**). Vanillin and H_3BO_3 resulted in both reduction of emission and a shift of emission wavelength. Side-by-side comparison of reactions with all reagents already exerted different reactivity patterns from different turmeric sources (**Figure 13**).

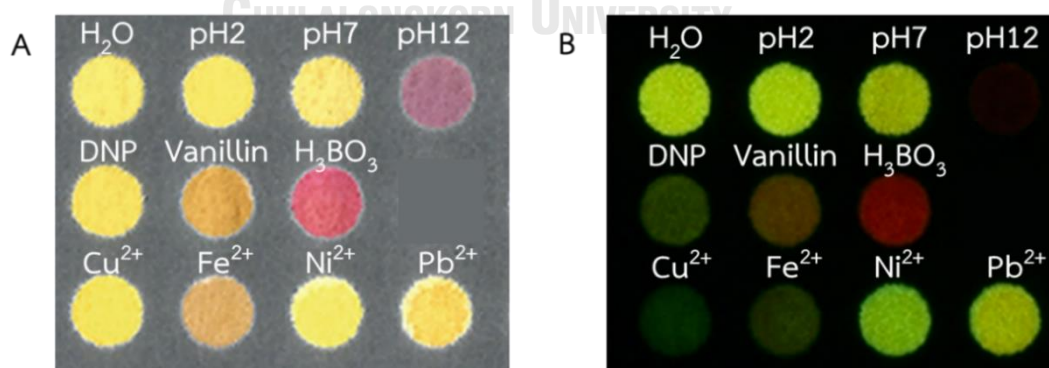


Figure 12 Paper arrays of chemical reactions probe after reacting with curcumin standard (**Cur11**) under (A) white light and (B) 365-nm UV light.

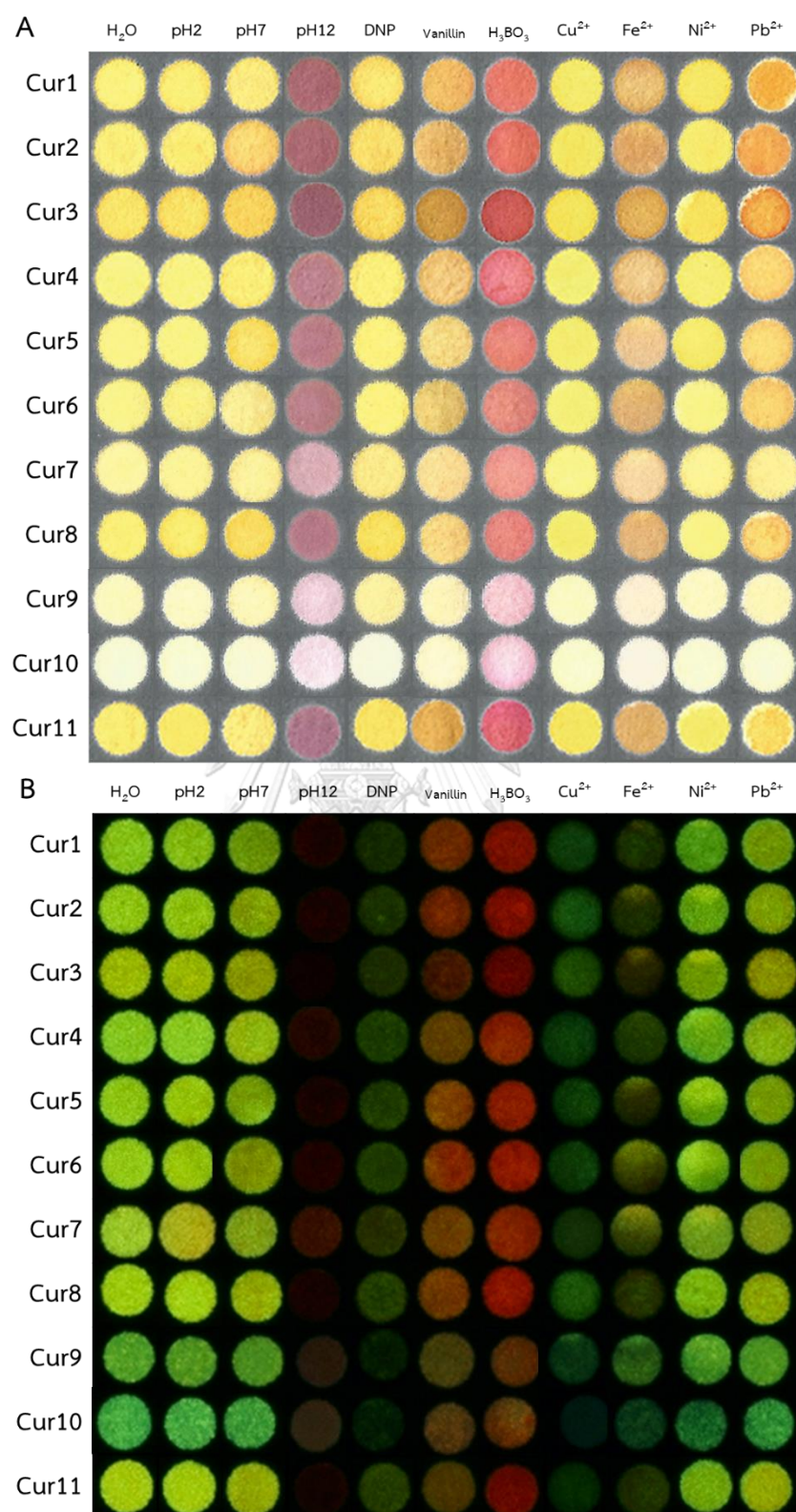


Figure 13 Paper arrays of chemical reactions probe after reacting with turmeric samples from all sources under (A) white light and (B) 365-nm UV light

To further confirm the potential of these reagents, further analyses were also conducted. First, a representative set of reaction arrays based on curcumin standard (**Cur 11**) was prepared, and the reaction profiles of the responses of this curcumin sample to selected reagents in digital images were converted into numerical data by ImageJ processing software. This was then plotted as bar graphs as shown in **Figure 14**. It is evident from these data that each reagent gave different responses, both as the total intensity values, and in each color channel. Furthermore, the limits of detection (LOD) of some reagents to the curcumin standard were also determined to give some general ideas of how sensitively each reagent responds to curcumins. As shown in **Figure 15-21**, various reagents gave various LOD around mid to high micromolar ranges, with a general trend being that the fluorescence responses unsurprisingly provided better sensitivities than did white-light responses. Anyway, it should be emphasized herein that the sensitivities may not be utmost important as this can be overcome by adding more turmeric samples into each reaction well. Instead, the fact that each reagent reacted differently (thus giving different LOD and slope profiles) was perhaps more essential.

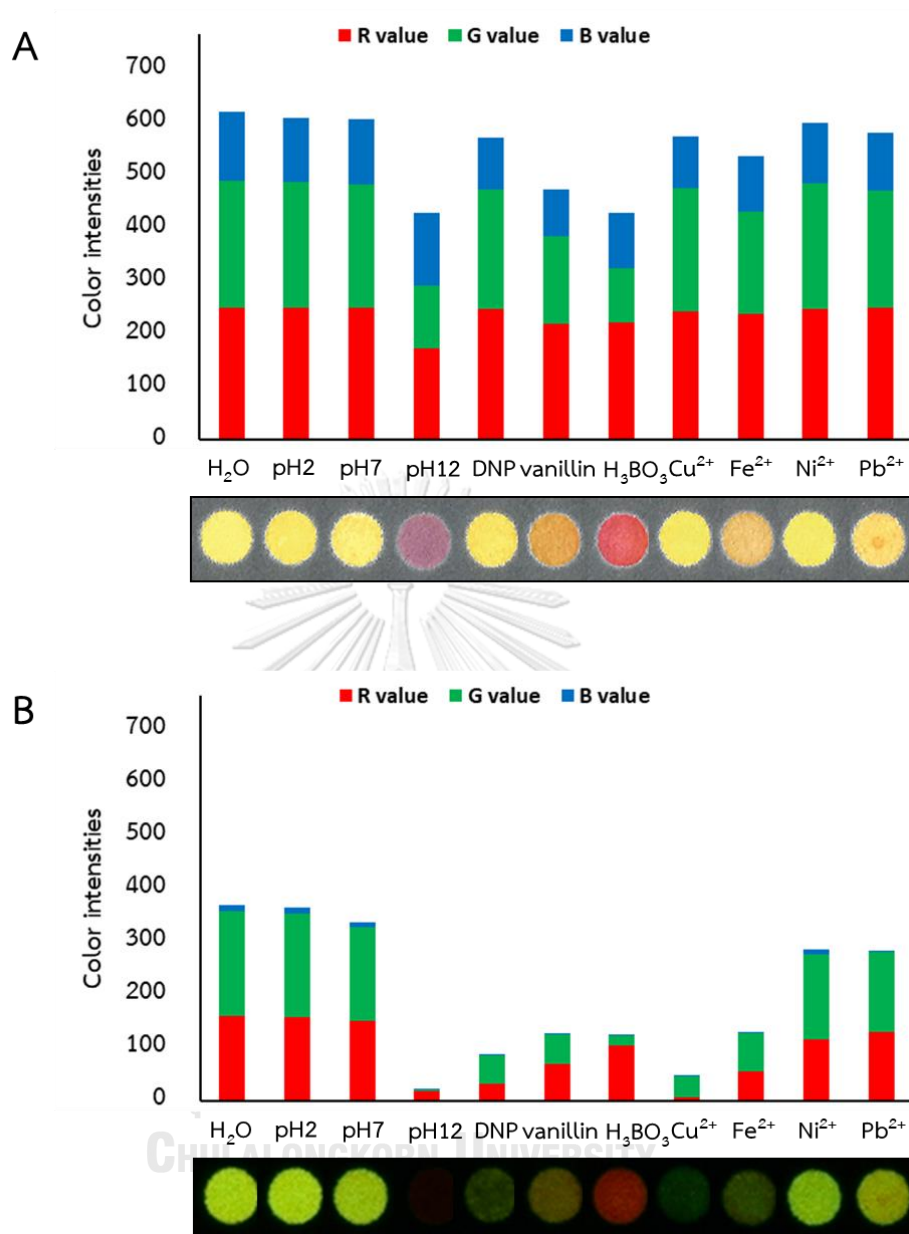
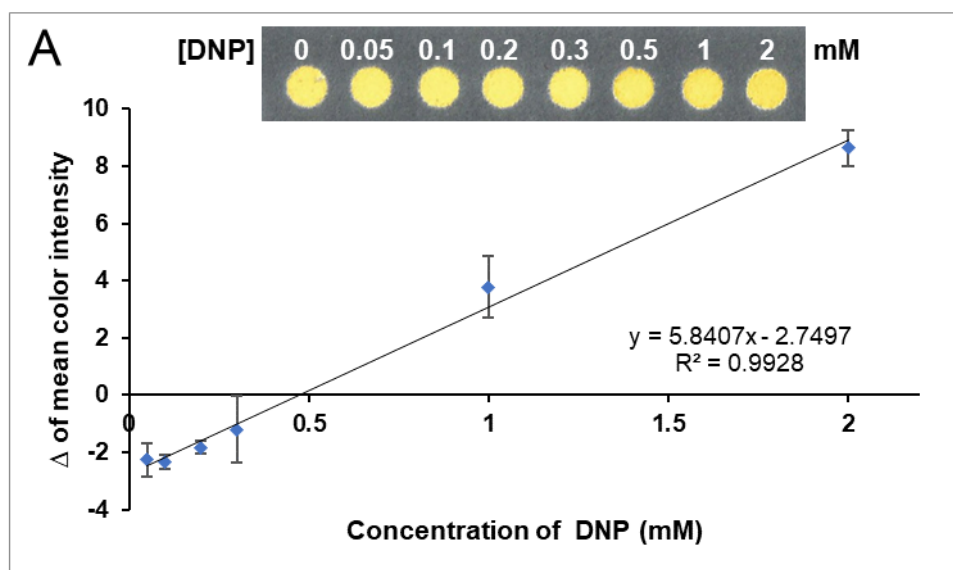
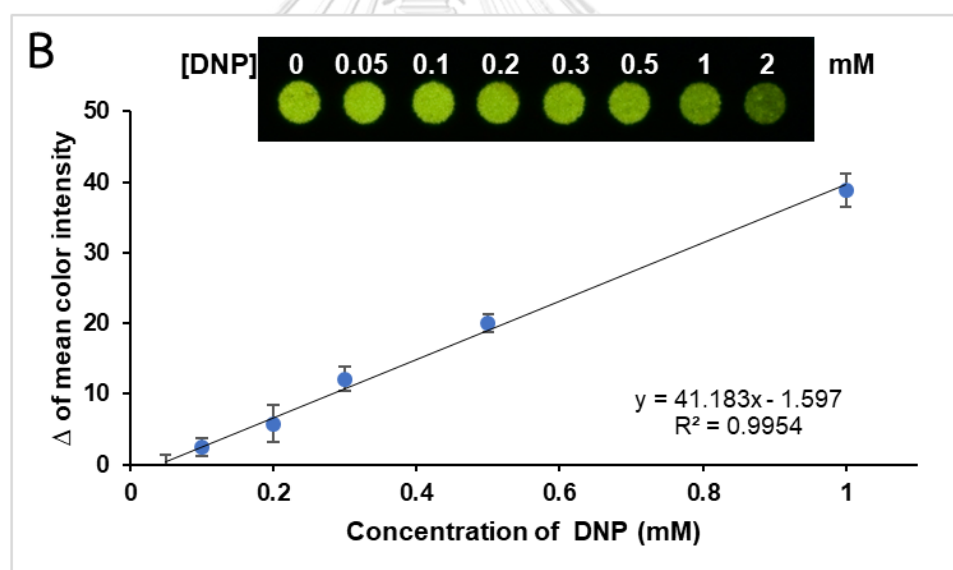


Figure 14 Colorimetric and fluorescence responses of paper arrays to various reagents after being exposed to 0.2-mM curcumin standard (**Cur11**) under (A) white light and (B) 365-nm UV light.

The maximum intensity value (y-axis) is 765, which is the combination of the maximum intensities of the three-color components (red, green, and blue).

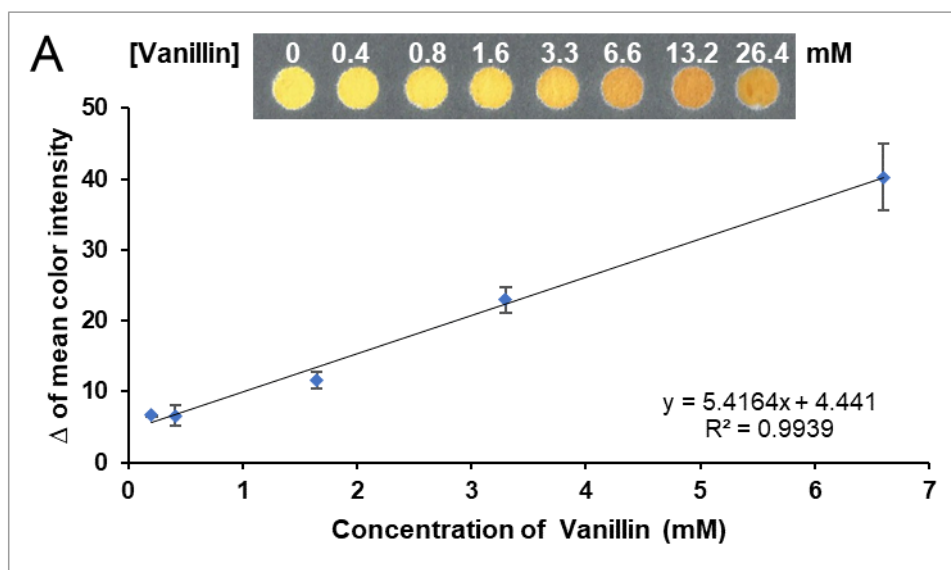


Limit of detection = $1.3 \times 10^{-4} M$

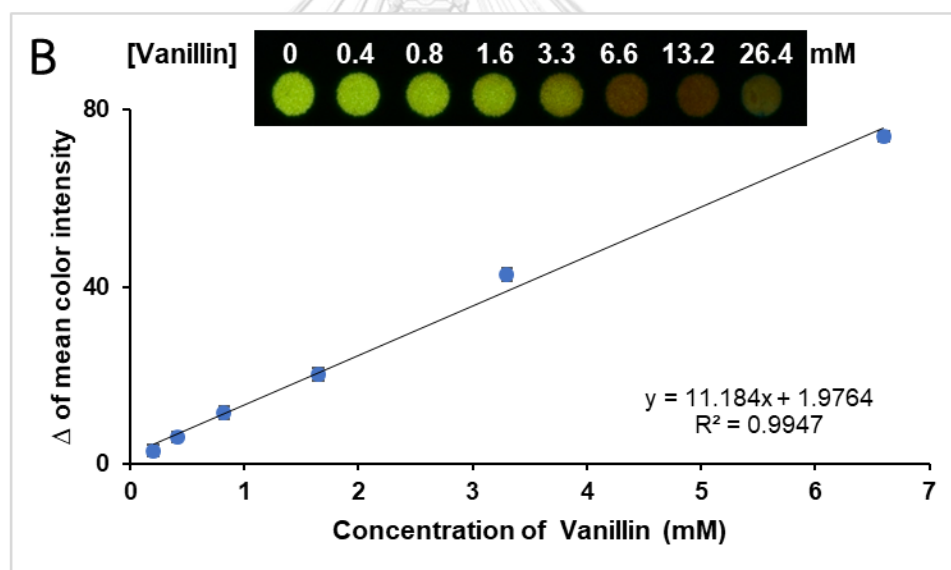


Limit of detection = $5.4 \times 10^{-5} M$

Figure 15 Colorimetric responses of curcumin standard (**Cur11**) with different concentration of DNP and calibration plots of the Δ of mean color intensity ($n = 3$) under **(A)** white light and **(B)** 365-nm UV light.

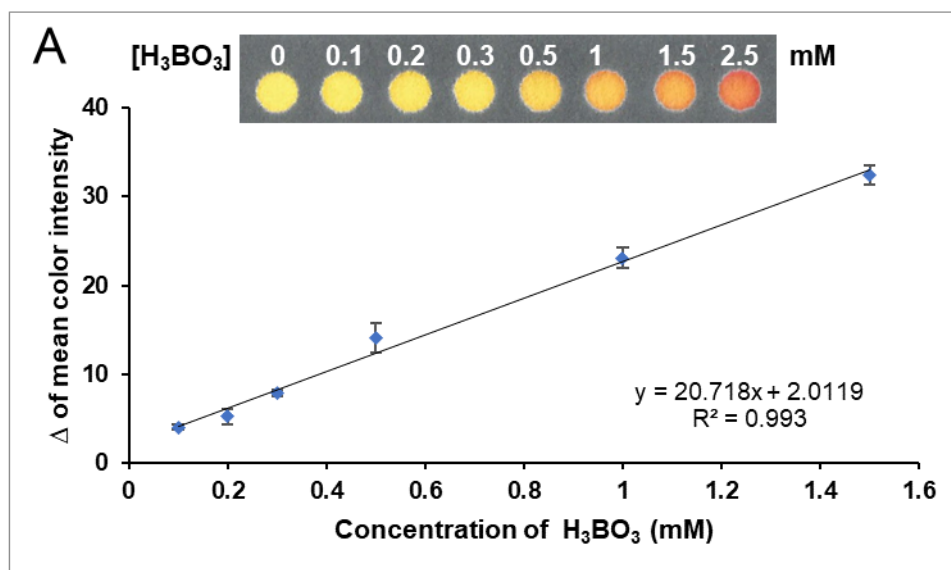


Limit of detection = 6.3×10^{-4} M

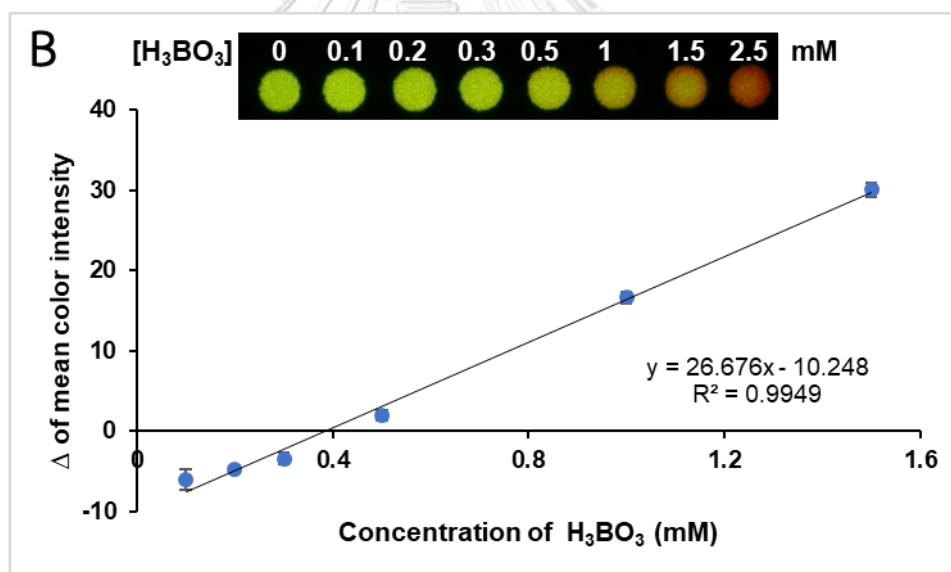


Limit of detection = 3.7×10^{-4} M

Figure 16 Colorimetric responses of curcumin standard (**Cur11**) with different concentration of vanillin and calibration plots of the Δ of mean color intensity ($n = 3$) under **(A)** white light and **(B)** 365-nm UV light.

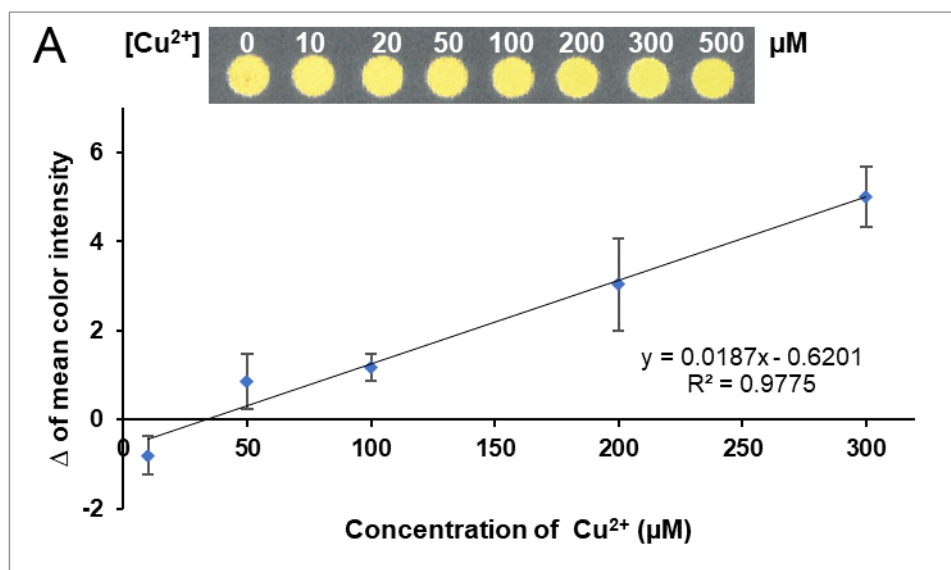


Limit of detection = 1.1×10^{-4} M

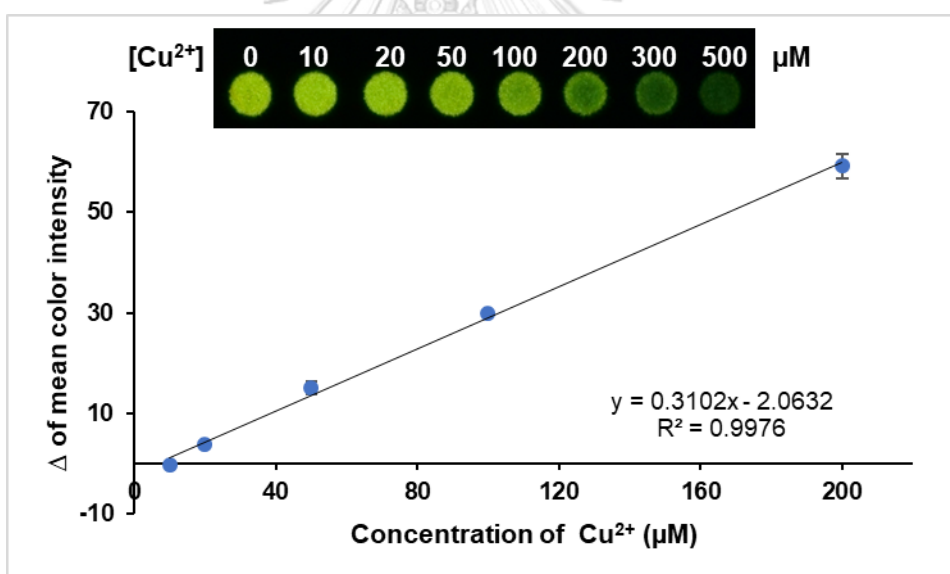


Limit of detection = 9.2×10^{-5} M

Figure 17 Colorimetric responses of curcumin standard (**Cur11**) with different concentration of H₃BO₃ and calibration plots of the Δ of mean color intensity ($n = 3$) under (A) white light and (B) 365-nm UV light.

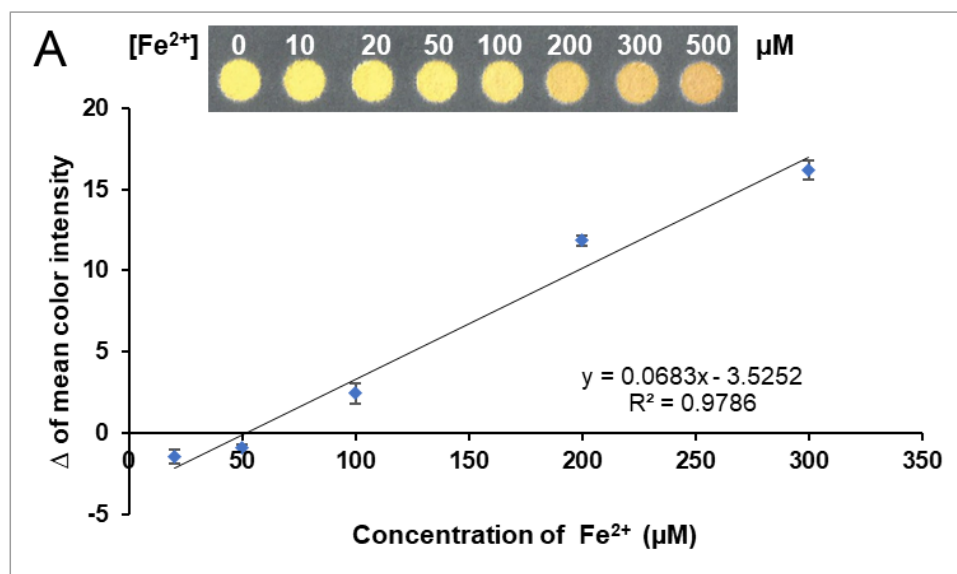


Limit of detection = $4.9 \times 10^{-5} \text{ M}$

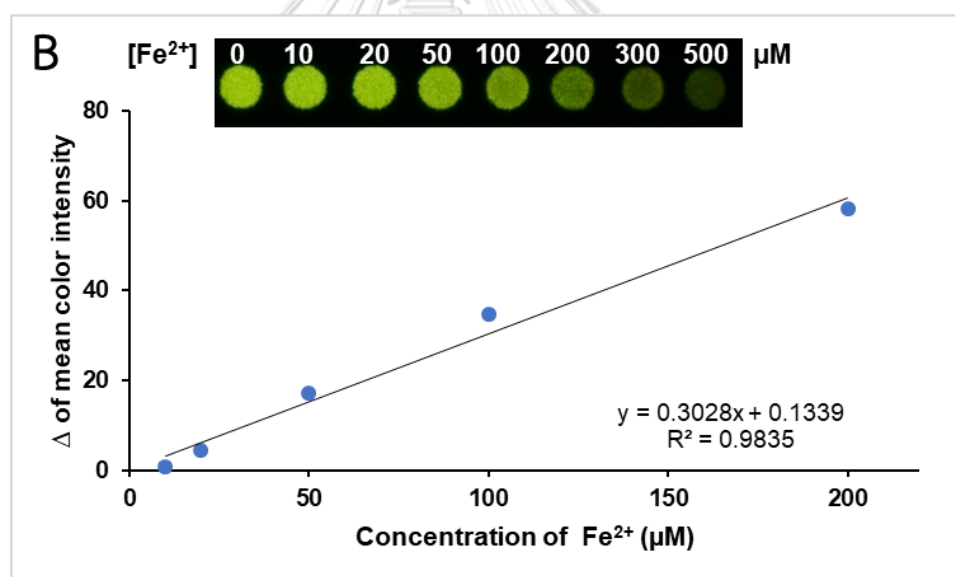


Limit of detection = $9.6 \times 10^{-6} \text{ M}$

Figure 18 Colorimetric responses of curcumin standard (**Cur11**) with different concentration of Cu²⁺ and calibration plots of the Δ of mean color intensity ($n = 3$) under **(A)** white light and **(B)** 365-nm UV light.

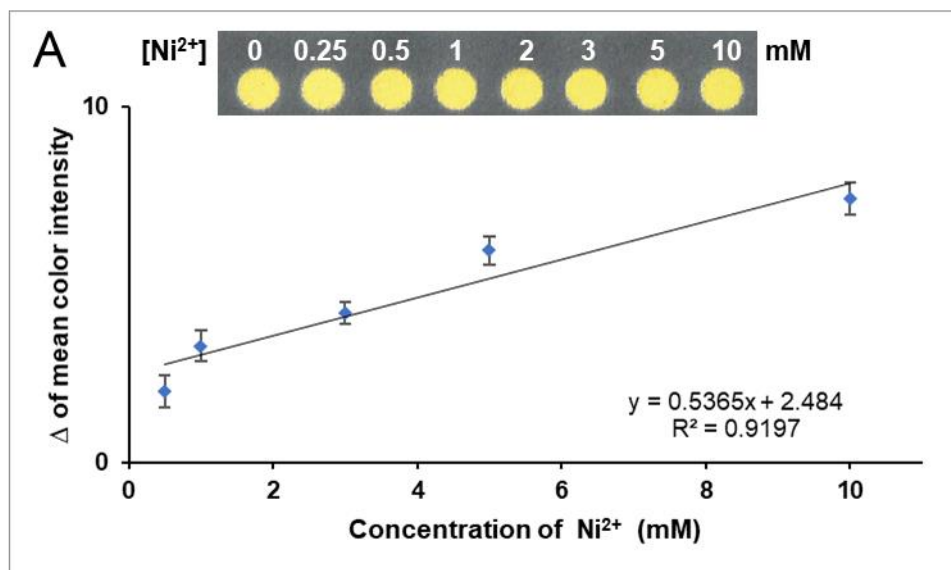


Limit of detection = $4.8 \times 10^{-5} \text{ M}$

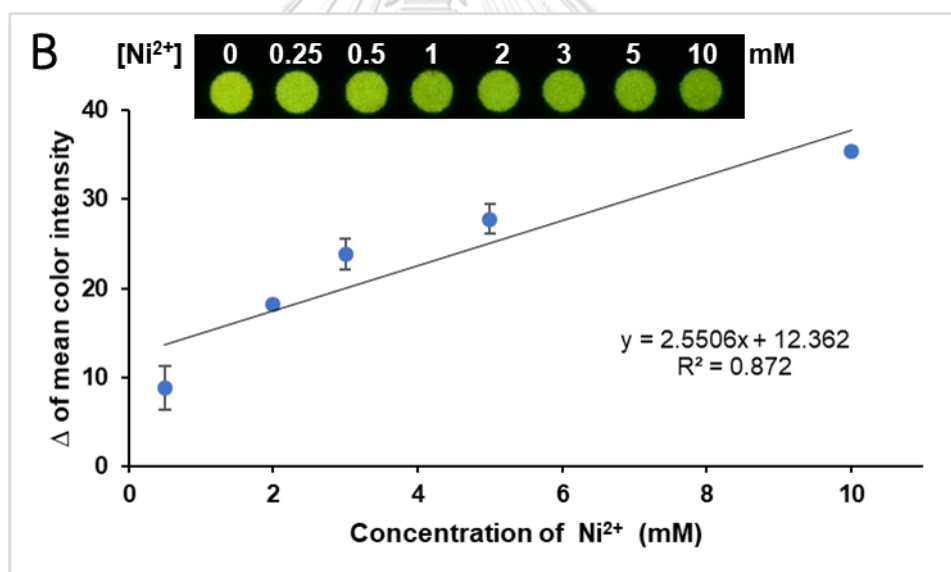


Limit of detection = $2.5 \times 10^{-5} \text{ M}$

Figure 19 Colorimetric responses of curcumin standard (**Cur11**) with different concentration of Fe²⁺ and calibration plots of the Δ of mean color intensity ($n = 3$) under (A) white light and (B) 365-nm UV light.

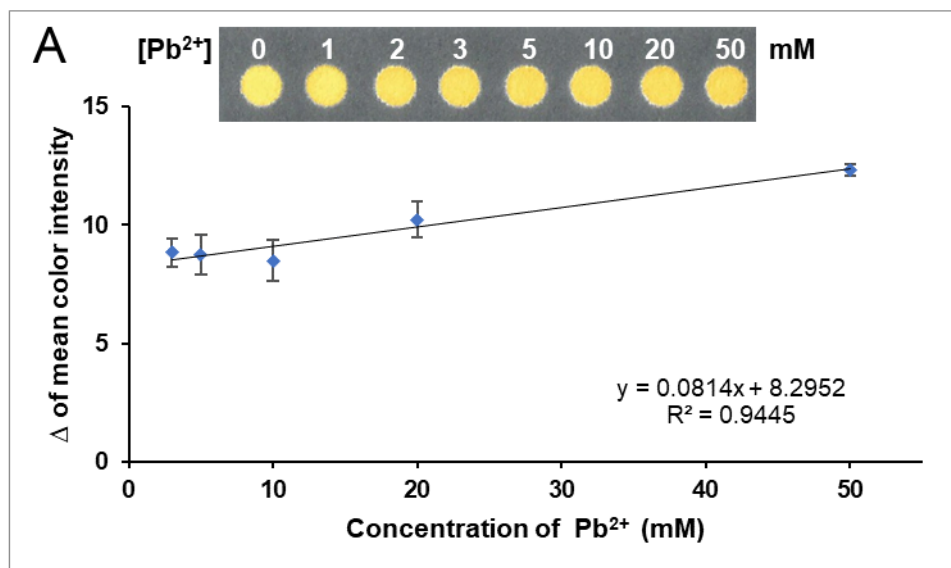


Limit of detection = $2.9 \times 10^{-3} M$

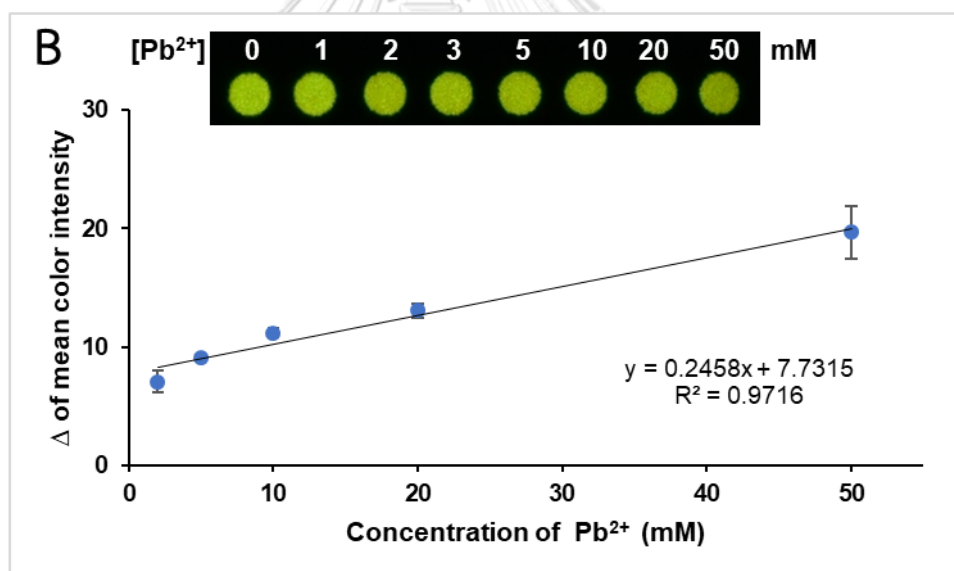


Limit of detection = $3.8 \times 10^{-3} M$

Figure 20 Colorimetric responses of curcumin standard (**Cur11**) with different concentration of Ni²⁺ and calibration plots of the Δ of mean color intensity ($n = 3$) under (A) white light and (B) 365-nm UV light.



Limit of detection = $1.1 \times 10^{-4} M$



Limit of detection = $8.0 \times 10^{-3} M$

Figure 21 Colorimetric responses of curcumin standard (**Cur11**) with different concentration of Pb²⁺ and calibration plots of the Δ of mean color intensity ($n = 3$) under (A) white light and (B) 365-nm UV light.

3.3 Chemometric analysis

To allow for practical differentiations, all data were subject to chemometric treatments. This could be done by first converting reaction profiles from digital photos into numerical data by ImageJ processing software. The resulting data in the form of red, green, and blue (RGB) numerical values on both visualization modes (white and UV lights) of each reagent spot were then used to create a multidimensional data set. This consisted of 99 samples (11 turmeric sources with 9 replicates) and 66 variables (3 RGB numerical data, 2 visualization modes and 11 reagent wells), which were then used to investigate the prediction accuracy of all possible combinations from the reagent arrays (2047 combinations). Most combinations gave the prediction accuracy of higher than 50% (**Figure 22**). Notably, the discovery of this best combination of reagents was made possible by the use of chemometrics, which permitted relatively rapid analysis on the prediction accuracies of all reagent combinations. This resulted in a set of 8 reagents (H_2O + pH2 + DNP + vanillin + H_3BO_3 + Fe^{2+} + Ni^{2+} + Pb^{2+}) that provided a satisfactorily maximum 93.9% prediction accuracy. Interestingly, the result from the maximum (eleven) combination gave lower prediction accuracy at about 73.7%, hence highlighting the utility of chemometric approach.

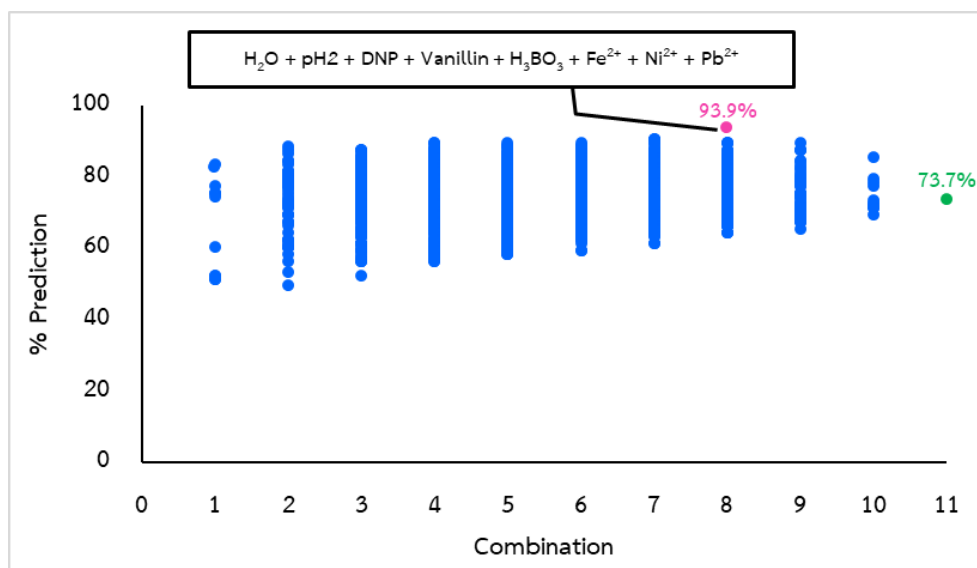


Figure 22 A plot between the percentages of prediction accuracies and the numbers of reagents used in the differentiation process.

To visualize the relation of samples, principal component analysis (PCA) was performed on the data using the aforementioned 8 selected reagents, along with the all (eleven) reagents condition as a comparison. Both PC plots of PC1 vs. PC2 (**Figure 23A**) and PC1 vs. PC3 (**Figure 23B**) for the eleven-combination provided clear differentiations on five samples, with the most prominent ones being **Cur9** from Myanmar and **Cur10** from China. Some indistinguishable samples were illustrated as filled items. As shown in **Figure 23A**, the most ambiguous sample was **Cur8** from India (shown as orange star) with six non-differentiable replicates. Interestingly, PC plots using data from the eight-combination (**Figure 24A** and **B**) showed clear discrimination on seven samples including **Cur8** (India) and **Cur3** (Singapore). However, there are some indistinguishable replicates in **Cur1**, **Cur2**, **Cur5** and **Cur6** which were from the same country (Thailand).

In essence, chemometric treatment aided in demonstrating the power of reagent arrays, where it unambiguously showed that combinations of reagents, but not just any individual reagent, were needed for better predictions on the geographical profiles of turmeric samples. On the contrary, chemometrics helped in reducing the time and effort of conducting experiments by clearly suggesting the

optimum set of experiments, which are not necessarily the ones with highest numbers of variables. This could be clearly illustrated in a heat-map chart in **Figure 25**. Matched colors on each row to the reference panel on the right panel indicated that those reagents (or combinations thereof) could correctly predict the origin of the sample. **Cur9** and **Cur10**, the most prominent samples from all PC plots had perfect geographical prediction although the single reagent was used. However, the other samples that accumulated on the right of all PC plots required the utilization of reagent combination for better predictions than single reagent. Clearly, the suggested 8-reagent combination obtained from chemometric treatment gave the highest number of matched colors, which was significantly higher than any individual reagent or even all reagents.



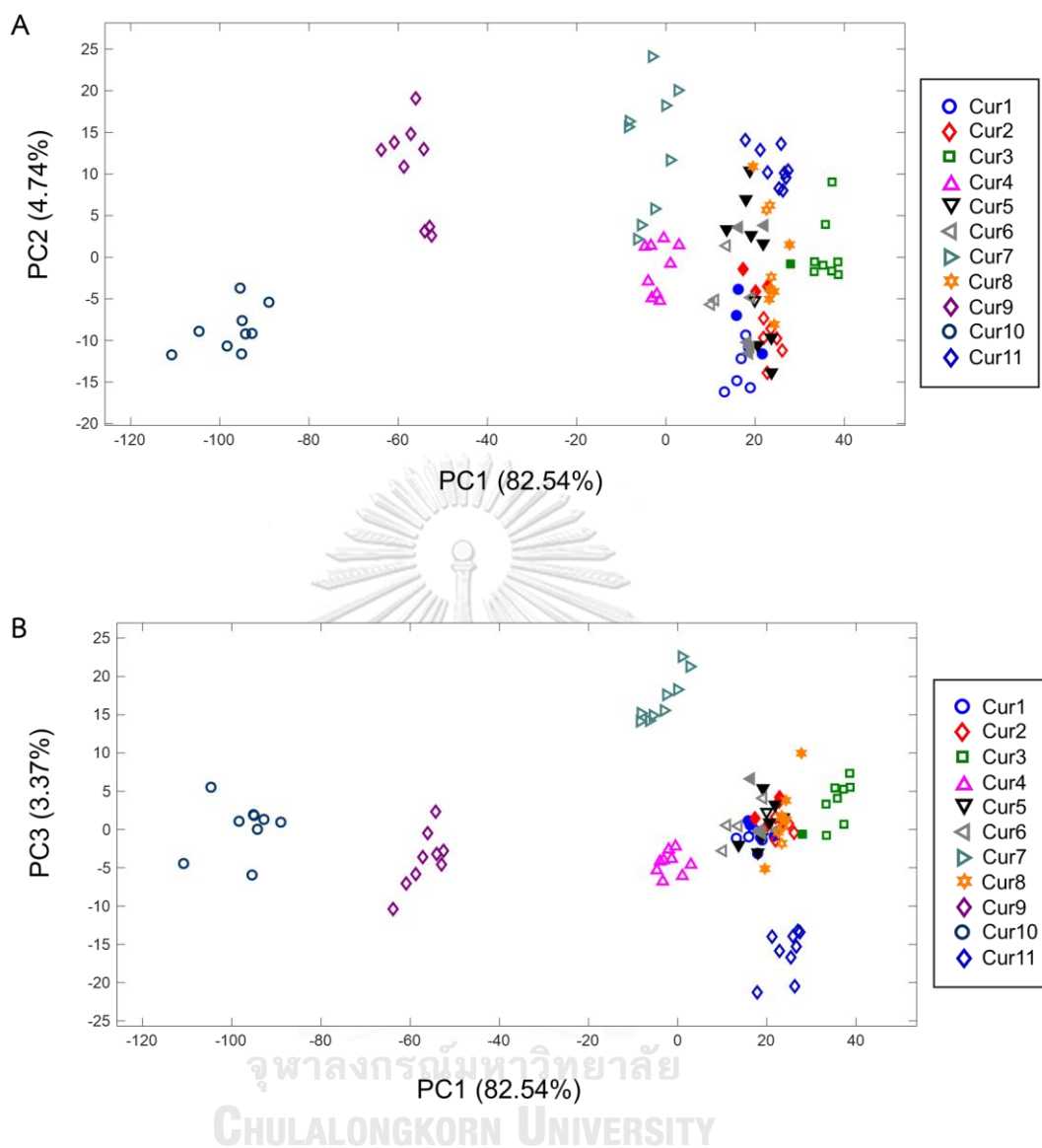


Figure 23 Two-dimensional PC score plots of (A) PC1 vs. PC2 and (B) PC1 vs. PC3 for the combination of all reagents in discriminating 11 turmeric sources. Filled items represented indistinguishable samples.

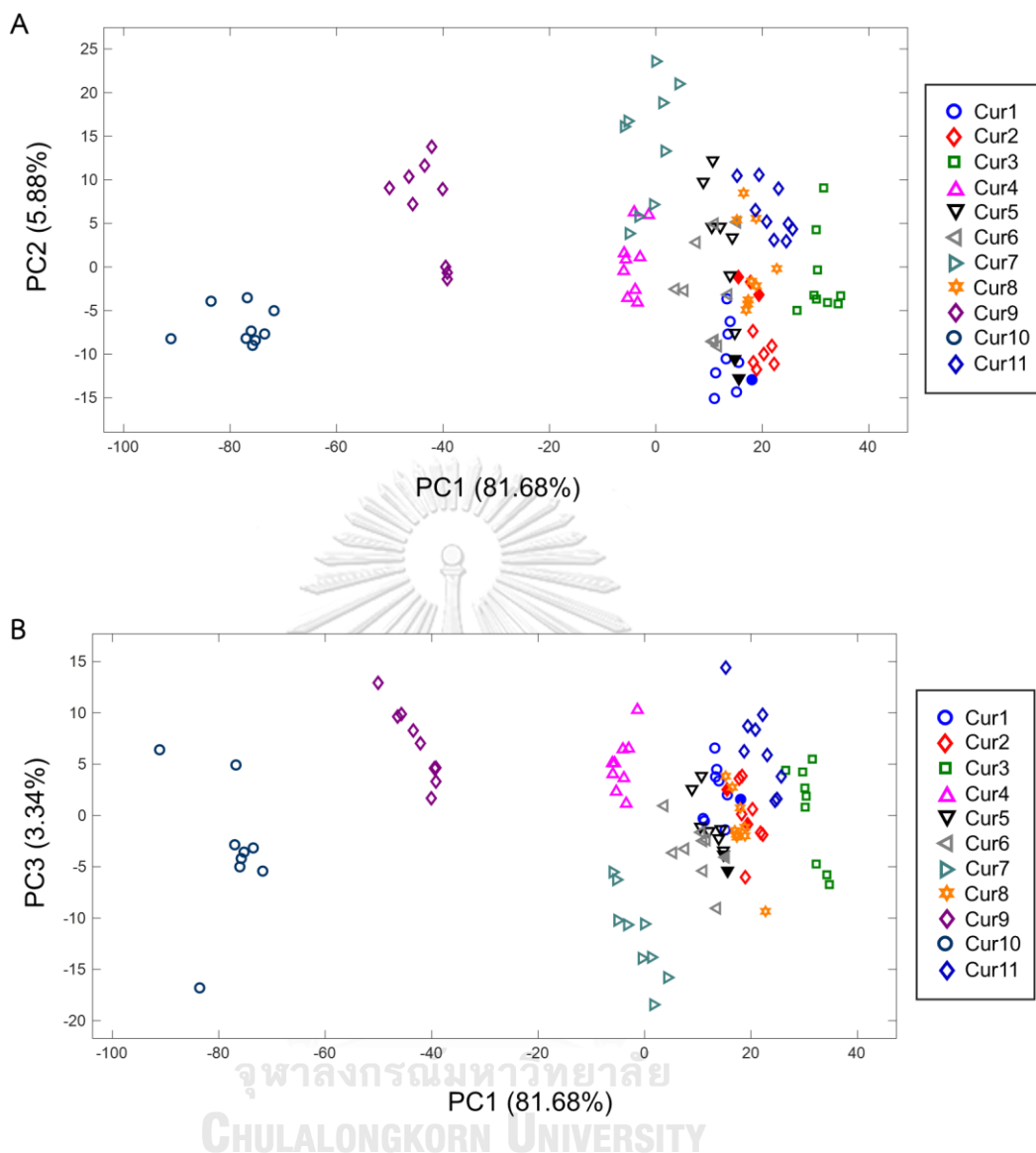


Figure 24 Two-dimensional PC score plots of (A) PC1 vs. PC2 and (B) PC1 vs. PC3 for the combination of 8 reagents ($H_2O + pH2 + DNP + vanillin + H_3BO_3 + Fe^{2+} + Ni^{2+} + Pb^{2+}$) in discriminating 11 turmeric sources. Filled items represented indistinguishable samples.



Figure 25 A heat-map chart as a representation of correctness in predicting the origins of turmeric samples.

(8 reagents were H₂O + pH2 + DNP + vanillin + H₃BO₃ + Fe²⁺ + Ni²⁺ + Pb²⁺).

CHAPTER IV

CONCLUSION

In conclusion, this project demonstrated the synergistic utilization of chemical arrays and chemometric approach in indicating the geographical origins of turmeric samples. This was from the key hypothesis that a specific ratio of chemical compositions in turmeric from each origin may affect the reactions with chemical sensors in different ways and result in different changes in color intensities and hues.

Our preliminary experiment relied on HPLC and LC-MS confirmed an existence of unique ratios of curcuminoids and sesquiterpenes in different samples. The paper-based chemical arrays were then successfully fabricated based on the chemical reactions of these components with eleven-reagent sensors. Without the need for sophisticated instruments, the characteristic colorimetric and fluorescence profiles of each turmeric sample were captured and transformed into numerical data. Combining with chemometrics, our method provided competent GI discrimination with up to 94% prediction accuracy from the set of 8 reagents including H₂O, pH 2 (acidic buffer), DNP, vanillin, H₃BO₃, Fe²⁺, Ni²⁺, and Pb²⁺.

Furthermore, this proof-of-concept approach is also theoretically applicable to other foods and plants having chromophores, thus underscoring the impact of this method on broader usages.

REFERENCES



จุฬาลงกรณ์มหาวิทยาลัย
CHULALONGKORN UNIVERSITY

1. Dogan, B.; Gokovali, U., Geographical indications: The aspects of rural development and marketing through the traditional products. *Procedia - Social and Behavioral Sciences* **2012**, *62*, 761-765.
2. Medeiros, M. d. L.; Passador, C. S.; Passador, J. L., Implications of geographical indications: a comprehensive review of papers listed in CAPES' journal database. *RAI Revista de Administração e Inovação* **2016**, *13* (4), 315-329.
3. Luykx, D. M. A. M.; van Ruth, S. M., An overview of analytical methods for determining the geographical origin of food products. *Food Chemistry* **2008**, *107* (2), 897-911.
4. Uríčková, V.; Sádecká, J., Determination of geographical origin of alcoholic beverages using ultraviolet, visible and infrared spectroscopy: A review. *Spectrochimica Acta Part A: Molecular and Biomolecular Spectroscopy* **2015**, *148*, 131-137.
5. Monahan, F. J.; Schmidt, O.; Moloney, A. P., Meat provenance: Authentication of geographical origin and dietary background of meat. *Meat Science* **2018**, *144*, 2-14.
6. Yudthavorasit, S.; Wongravee, K.; Leepipatpiboon, N., Characteristic fingerprint based on gingerol derivative analysis for discrimination of ginger (*Zingiber officinale*) according to geographical origin using HPLC-DAD combined with chemometrics. *Food Chemistry* **2014**, *158*, 101-111.
7. Kritiotti, A.; Menexes, G.; Drouza, C., Chemometric characterization of virgin olive oils of the two major Cypriot cultivars based on their fatty acid composition. *Food Research International* **2018**, *103*, 426-437.
8. Gerothanassis, I. P.; Troganis, A.; Exarchou, V.; Barbarossou, K., Nuclear magnetic resonance (NMR) spectroscopy: basic principles and phenomena, and their applications to chemistry, biology and medicine. *Chemistry Education Research and Practice* **2002**, *3* (2), 229-252.
9. Tomita, S.; Nemoto, T.; Matsuo, Y.; Shoji, T.; Tanaka, F.; Nakagawa, H.; Ono, H.; Kikuchi, J.; Ohnishi-Kameyama, M.; Sekiyama, Y., A NMR-based, non-targeted multistep metabolic profiling revealed l-rhamnitol as a metabolite that characterised apples from different geographic origins. *Food Chemistry* **2015**, *174*, 163-172.

10. Kharbach, M.; Kamal, R.; Marmouzi, I.; Barra, I.; Cherrah, Y.; Alaoui, K.; Heyden, Y. V.; Bouklouze, A., Fatty-acid profiling vs UV-Visible fingerprints for geographical classification of Moroccan Argan oils. *Food Control* **2019**, *95*, 95-105.
11. Urvieta, R.; Buscema, F.; Bottini, R.; Coste, B.; Fontana, A., Phenolic and sensory profiles discriminate geographical indications for Malbec wines from different regions of Mendoza, Argentina. *Food Chemistry* **2018**, *265*, 120-127.
12. Gorji-Chakespari, A.; Nikbakht, M. A.; Sefidkon, F.; Ghasemi-Varnamkhasti, M.; Brezmes, J.; Llobet, E., Performance comparison of Fuzzy ARTMAP and LDA in qualitative classification of Iranian *Rosa damascena* essential oils by an electronic nose. *Sensors* **2016**, *16* (5).
13. Ali, N.; Soheil, A.-E., A review of therapeutic effects of curcumin. *Current Pharmaceutical Design* **2013**, *19* (11), 2032-2046.
14. Prasad, S.; Gupta, S. C.; Tyagi, A. K.; Aggarwal, B. B., Curcumin, a component of golden spice: From bedside to bench and back. *Biotechnology Advances* **2014**, *32* (6), 1053-1064.
15. Priyadarsini, K., The chemistry of curcumin: From extraction to therapeutic agent. *Molecules* **2014**, *19* (12), 20091.
16. Burgos-Morón, E.; Calderón-Montaño, J. M.; Salvador, J.; Robles, A.; López-Lázaro, M., The dark side of curcumin. *International Journal of Cancer* **2010**, *126* (7), 1771-1775.
17. Nelson, K. M.; Dahlin, J. L.; Bisson, J.; Graham, J.; Pauli, G. F.; Walters, M. A., The essential medicinal chemistry of curcumin. *Journal of Medicinal Chemistry* **2017**, *60* (5), 1620-1637.
18. Mukerjee, A.; Sørensen, T. J.; Ranjan, A. P.; Raut, S.; Gryczynski, I.; Vishwanatha, J. K.; Gryczynski, Z., Spectroscopic properties of curcumin: Orientation of transition moments. *The Journal of Physical Chemistry B* **2010**, *114* (39), 12679-12684.
19. Patra, D.; Barakat, C., Synchronous fluorescence spectroscopic study of solvatochromic curcumin dye. *Spectrochimica Acta Part A: Molecular and Biomolecular Spectroscopy* **2011**, *79* (5), 1034-1041.

20. Boga, C.; Delpivo, C.; Ballarin, B.; Morigi, M.; Galli, S.; Micheletti, G.; Tozzi, S., Investigation on the dyeing power of some organic natural compounds for a green approach to hair dyeing. *Dyes and Pigments* **2013**, *97* (1), 9-18.
21. Kim, H.-J.; Jo Kim, D.; S N, K.; Hemalatha, K.; Raj, J.; ok, S.; choe, Y., Curcumin dye extracted from *Curcuma longa* L. used as sensitizers for efficient dye-sensitized solar cells. *International journal of electrochemical science* **2013**, *8*, 8320-8328.
22. Zhou, Y.; Tang, R.-C., Modification of curcumin with a reactive UV absorber and its dyeing and functional properties for silk. *Dyes and Pigments* **2016**, *134*, 203-211.
23. Pourreza, N.; Golmohammadi, H., Application of curcumin nanoparticles in a lab-on-paper device as a simple and green pH probe. *Talanta* **2015**, *131*, 136-141.
24. Lawrence, K.; Flower, S. E.; Kociok-Kohn, G.; Frost, C. G.; James, T. D., A simple and effective colorimetric technique for the detection of boronic acids and their derivatives. *Analytical Methods* **2012**, *4* (8), 2215-2217.
25. Bhat, M. P.; Madhuprasad; Patil, P.; Nataraj, S. K.; Altalhi, T.; Jung, H.-Y.; Losic, D.; Kurkuri, M. D., Turmeric, naturally available colorimetric receptor for quantitative detection of fluoride and iron. *Chemical Engineering Journal* **2016**, *303*, 14-21.
26. Raj, S.; Shankaran, D. R., Curcumin based biocompatible nanofibers for lead ion detection. *Sensors and Actuators B: Chemical* **2016**, *226*, 318-325.
27. Kowalski, B. R., Chemometrics. *Analytical Chemistry* **1980**, *52* (5), 112-122.
28. He, X.-G.; Lin, L.-Z.; Lian, L.-Z.; Lindenmaier, M., Liquid chromatography–electrospray mass spectrometric analysis of curcuminoids and sesquiterpenoids in turmeric (*Curcuma longa*). *Journal of Chromatography A* **1998**, *818* (1), 127-132.
29. Chao, I.-C.; Wang, C.-M.; Li, S.-P.; Lin, L.-G.; Ye, W.-C.; Zhang, Q.-W., Simultaneous quantification of three curcuminoids and three volatile components of *Curcuma longa* using pressurized liquid extraction and high-performance liquid chromatography. *Molecules* **2018**, *23* (7).
30. Gad, H. A.; Bouzabata, A., Application of chemometrics in quality control of Turmeric (*Curcuma longa*) based on Ultra-violet, Fourier transform-infrared and ¹H NMR spectroscopy. *Food Chemistry* **2017**, *237*, 857-864.

31. Jones, L. A.; Hancock, C. K.; Seligman, R. B., The reaction of 2,4-dinitrophenylhydrazine with some dicarbonyl compounds and α -substituted carbonyl compounds. *The Journal of Organic Chemistry* **1961**, *26* (1), 228-232.
32. Sarkar, S. K.; Howarth, R. E., Specificity of the vanillin test for flavanols. *Journal of Agricultural and Food Chemistry* **1976**, *24* (2), 317-320.
33. Grotheer, E. W., Spectrophotometric determination of boric acid in boron powder with curcumin. *Analytical Chemistry* **1979**, *51* (14), 2402-2403.
34. van Leeuwen, S. M.; Hendriksen, L.; Karst, U., Determination of aldehydes and ketones using derivatization with 2,4-dinitrophenylhydrazine and liquid chromatography–atmospheric pressure photoionization–mass spectrometry. *Journal of Chromatography A* **2004**, *1058* (1), 107-112.
35. Zhang, J. S.; Guan, J.; Yang, F. Q.; Liu, H. G.; Cheng, X. J.; Li, S. P., Qualitative and quantitative analysis of four species of Curcuma rhizomes using twice development thin layer chromatography. *Journal of Pharmaceutical and Biomedical Analysis* **2008**, *48* (3), 1024-1028.
36. Carrilho, E.; Phillips, S. T.; Vella, S. J.; Martinez, A. W.; Whitesides, G. M., Paper microzone plates. *Analytical Chemistry* **2009**, *81* (15), 5990-5998.
37. Uchiyama, S.; Inaba, Y.; Kunugita, N., Derivatization of carbonyl compounds with 2,4-dinitrophenylhydrazine and their subsequent determination by high-performance liquid chromatography. *Journal of Chromatography B* **2011**, *879* (17), 1282-1289.
38. Xu, G.; Wang, J.; Si, G.; Wang, M.; Xue, X.; Wu, B.; Zhou, S., A novel highly selective chemosensor based on curcumin for detection of Cu²⁺ and its application for bioimaging. *Sensors and Actuators B: Chemical* **2016**, *230*, 684-689.
39. Leung, M. H. M.; Pham, D.-T.; Lincoln, S. F.; Kee, T. W., Femtosecond transient absorption spectroscopy of copper(II)–curcumin complexes. *Physical Chemistry Chemical Physics* **2012**, *14* (39), 13580-13587.

VITA

NAME Monrawat Rauytanapanit

DATE OF BIRTH 13 May 1991

PLACE OF BIRTH Ratchaburi, Thailand

INSTITUTIONS ATTENDED Kasetsart University
Chulalongkorn University

HOME ADDRESS 147 Rimklongdan Road, Bang Kho, Chom Thong, Bangkok, Thailand 10150

PUBLICATION

1. M. Rauytanapanit, S. Suraritdechachai, T. Vilaivan, and T. Praneenarat, *Journal of Chemical Education*, 2020.
2. M. Rauytanapanit, K. Janchot, P. Kusolkumbot, S. Sirisattha, R. Waditee-Sirisattha, and T. Praneenarat, *Marine Drugs*, 2019, 17(6), 328-339
3. K. Janchot, M. Rauytanapanit, M. Honda, T. Hibino, S. Sirisattha, T. Praneenarat, H. Kageyama, and R. Waditee-Sirisattha, *Journal of Eukaryotic Microbiology*, 2019.
4. M. Rauytanapanit, T. Sukmanee, K. Wongravee, and T. Praneenarat, *RSC Advances*, 2018, 8(73), 41950-41955.
5. M. Rauytanapanit, A. Opitakorn, M. Terashima, R. Waditee-Sirisattha, and T. Praneenarat, *Colloids and Surfaces B: Biointerfaces*, 2018, 164, 42-49.
6. A. Opitakorn, M. Rauytanapanit, R. Waditee-Sirisattha, and T. Praneenarat, *RSC Advances*, 2017, 7(54), 34267-34275.

AWARD RECEIVED DPST Young Scientist Award 2019: Best Publication
DPST student conference on Science and Technology
2019 (DPSTcon2019)